



Cyclists' personal exposure to traffic-related air pollution and its influence on bikeability

Phuong T.M. Tran^{a,b}, Moshu Zhao^c, Kohei Yamamoto^c, Laura Minet^d, Teron Nguyen^b, Rajasekhar Balasubramanian^{a,*}

^a Department of Civil and Environmental Engineering, National University of Singapore, Singapore 117576, Singapore

^b The University of Danang - University of Science and Technology, 54 Nguyen Luong Bang Street, Lien Chieu District, Danang City, Viet Nam

^c Department of Geography, National University of Singapore, Singapore 117570, Singapore

^d Department of Civil and Mineral Engineering, University of Toronto, 35 St. George Street Toronto, Ontario M5S 1A4, Canada



ARTICLE INFO

Keywords:

Cycling index
PM_{2.5}
Black carbon
Land use regression model
Deep neural network
Singapore

ABSTRACT

Previous studies on bikeability/cycling index have explored factors that influence cycling in cities, and developed indicators to characterize a bicycle-friendly environment. However, despite its strong influence on cycling behavior, cyclists' exposure to traffic-related air pollution has been often disregarded. To close this knowledge gap, we propose a comprehensive bikeability index that comprises four sub-indices: accessibility, suitability, perceptibility, and prevailing air quality in the vicinity of cycling routes. We evaluate cyclists' exposure to fine particulate matter and black carbon, and used open-source data, land-use regression models, deep neural networks and spatial analysis. The application of the proposed bikeability framework reveals that the inclusion of air quality makes a significant difference when calculating bikeability index in Singapore and hence it merits serious consideration. We believe that the newly developed framework will convince city planners to consider the importance of assessing cyclists' exposure to airborne particles when planning cycling infrastructure.

1. Introduction

Urban mobility is undergoing transformative changes to achieve a sustainable future in cities. Active modes of transport such as walking and cycling and public transport provide substantial environmental, health and economic benefits compared to the use of motorized personal vehicles (Andersson et al., 2018; Lovelace et al., 2017; Mulley et al., 2013; Ryu et al., 2020; Sun et al., 2020). Additional benefits include climate change mitigation (Keall et al., 2018; Zahabi et al., 2016). Based on the data collected from London (UK), and Delhi (India), Woodcock et al. (2009) showed that substantial reduction in carbon dioxide emissions is possible by introducing a combination of increased active mobility and increased use of low carbon-emission motor vehicles, rather than implementing one of the two measures. One option to promote active mobility in cities is to provide favorable characteristics of the built environment where urban dwellers live and move without much hindrance (Aldred, 2019; Smith et al., 2017). It has been shown that such characteristics have a positive influence on travel behaviors of individuals and encourage them to switch to active travel modes (Handy et al., 2006; Winters et al., 2013).

Cycling is a green, sustainable, and healthy mode of urban transport that has been widely advocated worldwide. As cycling is

* Corresponding author.

E-mail address: ceerbala@nus.edu.sg (R. Balasubramanian).

Table 1
Literature review.

Study	Main goals	Indicator/Influence factors				Data measured
		Accessibility	Suitability	Perceptibility	Air quality	
1. Bikeability index development						
Harkey et al. (1998)	A bicycle compatibility index		Bike lane and paved shoulder, curb lane, parking lane, traffic, etc.			Subjective + Objective
Van Dyck et al. (2012) ¹	Cyclability index related to perceived neighborhood environmental attributes	Land use mix-diversity, proximity of destinations	Walking and cycling facilities, parking difficulty	Aesthetics		Subjective + Objective
Winters et al. (2013) ¹	Bikeability index as a spatial tool	Destination density, Connectivity of bicycle-friendly streets	Topography, Bike route			Objective + Subjective
Krenn et al. (2015) ¹	Bikeability index to assess the bicycle-friendliness of urban environments	Land-use mix	Cycling infrastructure, bicycle pathways, main roads, topography	Green and aquatic areas		Objective
Lin and Wei (2018) ¹	Assess bikeability by an analytic network process	Accessibility (network, destination, land use)	Available facility	Amenity (natural and build environment)	Perception on air quality	Objective + Subjective
Gu et al. (2018) ²	Measure street walkability and bikeability using open source data	Convenience (network and facility density, facility accessibility)	Safety (bike lane)	Comfort (tree shade, bike lane isolation)		Objective
Porter et al. (2019) ¹	Transportation and recreation bikeability indices	Residential density, population density, distance to transit.	Bicycle lanes	Parks, tree canopy coverage	Ozone level	Subjective + objective.
2. Investigations of individual sub-indices/ indicators						
Wahlgren and Schantz (2012) ¹	Assessment of bicycle commuters' perceptions.	Low 'directness' of the route.		Beautiful, green, safe route environments, traffic congestion.	Exhaust fumes	Subjective
Winters et al. (2016) ¹	Correlation between Bike score and journey to work by cycling	Destination score, connectivity score	Hill score, bike lane score			Subjective
Hankey et al. (2017) ⁴	Investigate population-level patterns in exposure during active travel	Bicycle and pedestrian traffic volumes			Exposure to particulate concentrations	Objective
Saghapour et al. (2017) ¹	Measure cycling accessibility	Land uses diversity, number of activities, the travel impedance				Objective
Vedel et al. (2017) ¹	Investigate bicyclists' preferences.	Stops, travel distance.	Designated cycle track, road type	Crowding, environment, green surroundings		Subjective
Berger and Dörzapf (2018) ³	Identify stressful events on a bicycle ride by sensor technology			Perception and emotion of riders		Objective
Nielsen and Skov-Petersen (2018) ¹	Assess the significance of bikeability variables on the probability of cycling	Density/accessibility, regional position of area	Transport infrastructure			Subjective
Wu et al. (2019) ¹	Measuring the cycling destination accessibility of metro station areas.	Accessibility (work, residence, commercial, park, leisure, public transportation accessibility)				Objective
Kang et al. (2019) ¹	Explore the attributes of perceived bikeability	Convenience (accessibility and connectivity),	Safety	Pleasantness		Subjective
Pritchard et al. (2019) ³	Test the applicability of bicycle level of service rating schemes		Bicycle level of service			Subjective
Marquart et al. (2020) ¹	Decision-makers awareness on cyclists' needs and perceptions			Perceived environment		Subjective
3. Cycling related studies in Singapore, not relevant to index development						

(continued on next page)

Table 1 (continued)

Study	Main goals	Indicator/Influence factors				Data measured
		Accessibility	Suitability	Perceptibility	Air quality	
Meng et al. (2014) ¹	Investigate cycling level	Urban structure, transport policy	Bike infrastructure, Public transport			Subjective
Koh and Wong (2015) ¹	Evaluate non-motorised transport demand against supporting environment	Accessibility, capacity of the non-motorised transport networks	Safety			Subjective
Meng et al. (2016) ¹	Effects of weather conditions on cycling travel behavior			Weather conditions, weather forecast		Subjective
Terh and Cao (2018) ¹	GIS-based multi-criteria decision analysis framework for the support of cycling paths planning	Pedestrian traffic, institutions, facility, retail amenities, employment areas, MRT/LRT stations, bus stops	Slope, major roads			Subjective + Objective
Zhu and Zhu (2019) ³	Use cycling comfort index to measure the cycling comfort			Cycling comfort		Objective

Subjective measures: e.g., collection of data through community surveys.

Objective measures: e.g., data collected in the field or from existing land use databases available in geographic information system (GIS).

1, 2, 3, and 4: Unit of analysis following area, street segment, road segment and block.

LUR: Land Use Regression model.

cheap, fast, reliable and requires little space investments, it can be viewed as an efficient mode of transport compared to motorized transport (Börjesson and Eliasson, 2012). The concept of “bikeability”, “cyclability” or “cycling” index (these terms are used interchangeably) has recently been applied to assess a community’s cycling-related environment (Gholamialam and Matisziw, 2019; Nielsen and Skov-Petersen, 2018; Porter et al., 2019) with the underlying objective to compare different urban areas and point out specific landscapes that are most in need for improvement (Krabbenborg, 2015).

Many studies on bikeability have investigated factors influencing cycling as the preferred mode of active transport in cities, and developed indicators to characterize a bicycle-friendly environment from different perspectives. Accessibility, suitability and perceptibility have been widely studied to promote bikeability in cities (Lin and Wei, 2018; Saghpour et al., 2017; Wahlgren and Schantz, 2012; Winters et al., 2013). However, air quality, especially personal exposure (PE) to traffic-related air pollution (TRAP), has received insufficient attention in the evaluation of bikeability (Marquart et al., 2020; Zhao et al., 2018). A recent study pointed out that cyclists who receive information on short-term impacts of TRAP are concerned about avoiding maximum exposure to harmful air pollutants such as particulate matter (PM) (Anowar et al., 2017). In fact, exposure to TRAP during active travel has been linked to a number of negative health effects such as cardiovascular, respiratory diseases, cancer, and adverse birth outcomes (Krzyżanowski et al., 2005; Qiu et al., 2019; Raza et al., 2018). Therefore, integrated evaluation of cycling index should consider both physical environmental attributes and cyclists’ exposure to TRAP. The revised cycling index will in turn encourage urban planners, designers, and regulators to plan, design and manage cycling infrastructure in such a way that active mobility can still take place in cities with no adverse health impacts on cyclists.

In this paper, we propose a new bikeability framework that considers not only physical cycling indicators but also personal exposure of cyclists to fine particulate matter ($PM_{2.5}$) and black carbon (BC), the key components of TRAP. The focus is to assess the role of air quality as a contributor to the bikeability framework by varying its contribution to bikeability indices that have been recently developed worldwide. We take advantage of open-source data (such as land use map, road network, Google Street View (GSV) imagery) and make use of land-use regression model (LUR), deep neural network (SegNet) and Geographic Information System (GIS) techniques to assess and evaluate the proposed bikeability framework in a neighbourhood of Singapore as a case study.

2. Literature review

2.1. Bikeability index development

The bikeability index has been studied for a long time with indicators ranging from a single index to multiple sub-indices (see Table 1). Harkey et al. (1998) initially developed a bicycle compatibility index based on nine components of suitability (e.g., bike lane and paved shoulder, curb lane/sidewalk, parking lane, traffic, etc.). The sub-index, suitability, was discussed by Winters et al. (2013) as the availability of bike routes or designated cycle tracks which facilitate cycling activities. The significance of this index was mentioned by Lin and Wei (2018) in their study. Cycling suitability also considers hilliness and topography, which is usually inversely associated with cycling frequency (Krenn et al., 2015; Winters et al., 2013). Winters et al. (2013) added accessibility as a sub-index (destination density and connectivity of bicycle – friendly streets), together with suitability, to expand the scope of the bikeability index with balanced weights for all parameters. Since accessibility is considered as the ease of access to a desirable destination, it is closely related to the land-use patterns that make the destinations more accessible by cycling (Lin and Wei, 2018; Van Dyck et al.,

2012).

Further efforts included the third sub-index, perceptibility, based on the recommendation by Krenn et al. (2015) by considering green and aquatic areas. Lin and Wei (2018) proposed amenity (natural and build environment) while Gu et al. (2018) paid attention to comfort (tree shade, bike lane isolation). Porter et al. (2019) considered parks and tree canopy coverage as favourable factors. Perceptibility often includes factors that encourage cycling based on the location and characteristics of urban greenery. Finally, air quality represents the recent addition to the bikeability index as proposed by Lin and Wei (2018) while considering bicycle commuters' perceptions on air quality as part of amenity/perceptibility. The association between air quality and bikeability received more attention after Porter et al. (2019) reported their observations that the level of ozone in ambient air was found to be inversely correlated with bicycling frequency. However, the PE of cyclists to PM of traffic origin is seldom considered and hence our interest in the subject matter addressed in this manuscript.

2.2. Investigation of individual sub-indices and indicators

Besides the main purpose of bikeability index development, more dedicated studies were conducted over the past five years (Table 1) to evaluate the effects of individual indicators/factors on the bikeability, or active travel behavior. Accessibility has attracted more interests in recent years. Saghpour et al. (2017) assessed the cycling accessibility from the viewpoints of land uses diversity, the range of activities, and the travel impedance. Wu et al. (2019) measured the cycling accessibility with reference to specific destinations based on attributes of work, residential, commercial, and park locations. The effect of suitability on bikeability was studied based on the consideration of (a) bike/transport infrastructure (Meng et al. (2014), Nielsen and Skov-Petersen (2018)); (b) topology (Terh and Cao (2018), Winters et al. (2016); and (c) safety (Kang et al. (2019), Koh and Wong (2015)). Among these factors, the lack of safety is a main deterrent for cycling. According to a study by Kang et al. (2019), "all participants felt "safe" when bikeways were separated from motorized traffic, or pedestrians", and "all study participants reported experiencing one or more safety threats and high fatigue" while riding cycles on mixed traffic roads.

The perception of cyclists on the surrounding environment was studied by Berger and Dörrzapf (2018), Marquart et al. (2020), Vedel et al. (2017) and Wahlgren and Schantz (2012). While green spaces, tree shades, and night lighting are found to be influencing factors that encourage cycling, traffic congestion and crowdedness have an opposite impact on cycling (Wahlgren and Schantz, 2012). Finally, the effect of exhaust fumes on bicycle commuters' perceptions was investigated by Wahlgren and Schantz (2012) and that of exposure to particulate concentrations on population-level travel patterns was investigated by Hankey et al. (2017). While the exposure to exhaust fumes was found to discourage cycling (Wahlgren and Schantz, 2012), it is interesting to observe that active travel (both cycling and walking) often occurs on high-traffic streets, or near activity centers where particulate concentrations are highest (Hankey et al., 2017). This trade-off between the frequency of active travel and the high concentration of PM merits a serious consideration, which has motivated this study.

The development of bikeability and the factors that influence cycling behavior are locally dependent (see Table 1). Studies on cycling have been conducted mostly in Western Europe, North America (e.g., Nielsen and Skov-Petersen, 2018; Pritchard et al., 2019; Wahlgren and Schantz, 2012; Winters et al., 2013, 2016), China and Japan (Day, 2016; Lin et al., 2018; Zhang et al., 2017; Zhao, 2014; Zhao et al., 2015). Such efforts to promote cycling as an active mode of transport are still sparse in countries within South-East Asia (SEA). SEA is a subregion of Asia, consisting of 11 countries and having about 8.5% of the world population (ASEAN, 2020). Air pollution burden caused by PM in SEA is reported to be among the highest in the world (Brauer et al., 2016; WHO, 2018). Given the difference in urban characteristics, traffic volume/composition, weather and air quality conditions within SEA, systematic studies on the PE of cyclists to TRAP are warranted. Singapore, being one of the most densely populated urbanized areas with mixed land-use characteristics, can be used as a testbed because it wishes to remain as a smart and sustainable nation despite the high population density (~7800 people/km²) (Nguyen et al., 2019a, 2019b). Particulate pollution is of major concern in terms of air quality in Singapore, in which transport contributes about 50% of the ambient PM_{2.5} levels due to vehicular exhaust emissions (MOT, 2020; Tran et al., 2020a, 2020b). Cycling only constitutes a very small proportion (1–2%) of transportation in Singapore. It is mostly used for short trips as part of the daily journey to work, typically to the Mass Rapid Transit (MRT) station or bus interchange, or for intra-town travels (Koh and Wong, 2015). The government has put forth a lot of efforts to promote Singapore as a bicycle-friendly city, such as the National Cycling Plan, which aims to expand bicycling infrastructure to over 1000 km in length by 2040 (LTA, 2018). However, the effects of air pollution on cycling have not been systematically investigated in Singapore (Meng et al., 2016). A quantifiable evaluation of the current cycling network through a comprehensive cycling index can guide local actions to stimulate an increase in the cycling mode of travel, and this initiative will encourage other countries within SEA to emulate Singapore.

Among 23 recently published articles listed in Table 1, 19, 14, 12, and 4 studies are related to accessibility, suitability, perceptibility and air quality, respectively. However, only two studies by Hankey et al. (2017) and Porter et al. (2019) measured air pollution effects objectively, the other two studies by Wahlgren and Schantz (2012) and Lin and Wei (2018) qualified the perception of cyclists on air quality subjectively. In short, the following three knowledge gaps motivated this study:

- (1) The importance of air quality in the assessment of bikeability has gained more interest in recent years, given the trade-off between high levels of active mobility in the urban location and high concentrations of airborne particles (Hankey et al., 2017);
- (2) The study by Porter et al. (2019) considered ozone levels in ambient air in the development of bikeability; however, ozone was measured at fixed air quality monitoring stations which do not directly reflect cyclists' PE to air pollutants. Many studies have revealed that fixed air quality monitoring stations significantly underestimate the exposure of city dwellers to TRAP in transport microenvironments (Adam et al., 2020; Kaur et al., 2007; Tran et al., 2020a, 2020b); and

- (3) To the best of our knowledge, no comprehensive study has been conducted in SEA to evaluate cyclists' exposure to TRAP and include near-road air quality as a sub-index of bikeability despite having a high population density.

The important research question to be addressed is: Is the cyclists' exposure to TRAP a significant component of the bikeability/cyclability index? The findings from this comprehensive research study will help city planners and environmental policymakers, not only in Singapore but also worldwide, to consider the importance of cyclists' PE to airborne particles when planning cycling infrastructure. The conventional approach towards cyclability is to improve the cycling infrastructure and to inform the public where to go cycling. To address the research question, we propose a new framework with incorporation of air quality sub-index into bikeability index and describe the related methodology in detail below. We conducted sensitivity analysis to evaluate the significance of air quality's contribution to bikeability indices developed worldwide. We have made use of open-source data, LUR models, SegNet and GIS techniques.

3. Methodology

3.1. Proposed bikeability framework

To evaluate the influence of air quality on bikeability/cyclability, four sub-indices are incorporated into the proposed framework in Fig. 1, including air quality, accessibility, suitability, and perceptibility. These indices were selected based on a thorough literature review of past studies conducted overseas and in Singapore (Table 1). In our study, the air quality work focuses on the assessment of PE of cyclists to PM_{2.5} and BC over the road network. BC is a light-absorbing component of PM_{2.5}, emitted by the incomplete combustion of fossil fuels, biomass or any carbon-containing matter (Andreae and Gelencsér, 2006; Menon et al., 2002; Rizzo et al., 2013; Sharma et al., 2010). The toxicity of PM_{2.5} and BC makes them good indicators of potential adverse health effects of airborne particles from traffic-related emission sources. Accessibility denotes a density of potential cyclists' destinations (grouped in leisure, transport, commercial and daily routine), while suitability is characterized by the slope, sinuosity and bike route. Perceptibility is assessed based on the greenery, crowdedness and outdoor enclosure. All details of sub-indices and indicators calculation are described in Sections 3.3–3.5. All indicators used in the framework are objective and quantitative.

In Table 1, data measurement methods are classified into objective, subjective, and a combination of both objective and subjective approaches with 7, 10, and 6 related studies, respectively. Each method has its own advantages and disadvantages. The so-called subjective measures account for roughly half of the total number of studies. The desired physical environmental characteristics

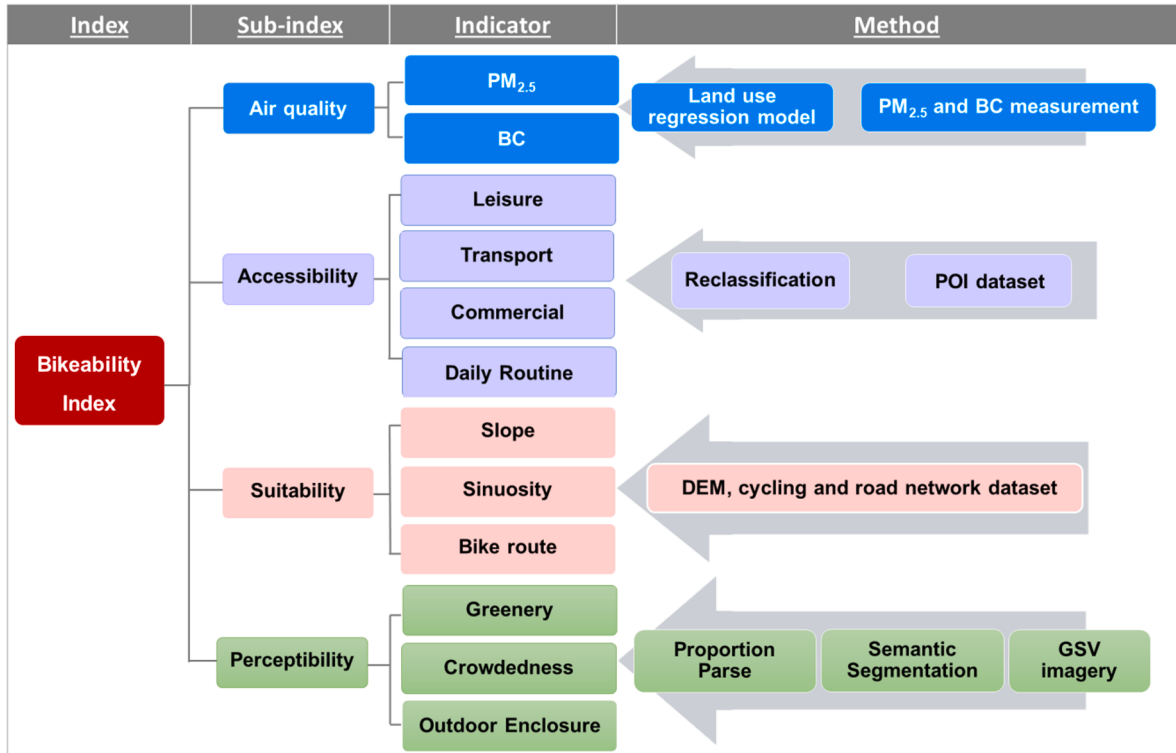


Fig. 1. Proposed framework for the evaluation of the bikeability index. (PM_{2.5}: particulate matter with size less than 2.5 μm in aerodynamic diameter, BC: black carbon, DEM: digital elevation model, POI: point of interests, GSV: Google Street View).

have been collected mainly through community surveys (Nielsen and Skov-Petersen, 2018; Vedel et al., 2017; Wahlgren and Schantz, 2012), which are subject to limitations in terms of sample size and site coverage. However, some studies have used objective data, such as data collected in the field or from existing land use databases available in GIS that can extrapolate results widely and rapidly in city-scale network (Gu et al., 2018; Saghafpour et al., 2017). It should be noted that this method is not suitable for assessing subjective parameters such as perceived risks and perceived safety along cycling routes. By using a combination of objective and subjective measures, researchers can take advantage of the merits of the two previous methods and deal with their shortcomings at the same time (Terh and Cao, 2018; Ueberham et al., 2019).

In our study, we attempted to overcome the disadvantage of the subjective approach by utilizing available land use maps, road networks, LUR models and GIS spatial analysis. Statistical R software (version 4.0.1) was used to develop LUR models and ArcGis pro (version 2.5.0) was used for spatial analysis. To quantify all the objective parameters related to cyclists' perception of greenery, crowdedness and outdoor enclosure, recent and innovative deep learning SegNet is used to analyze GSV imagery based on Python programming (version 3.8.2). The method proposed by Zhou et al. (2019) to calculate the pedestrians' perceptibility for each road site was employed for assessing cyclists' perceptibility in this study, given the similarity between these two active travel modes in terms of being human-powered and environmental friendly. Besides, as vulnerable users, both cyclists and pedestrians are directly in contact with the surrounding environment and experience prevailing weather conditions. They also cover short travel range at low speed as a part of multimodal transport (Muhs and Clifton, 2016; Nielsen and Skov-Petersen, 2018).

3.2. Study site and description of data sources

This paper uses the Western Region (WR) of Singapore as a case study for the evaluation of the bikeability index using the proposed framework. WR is one of the five regions in the city-state with the largest (about 201.3 km²) and the second most populated (914,570 residents in 2015) land area (Department of Statistics Singapore, 2020). Fig. 2 shows the location, districts and land use map of the WR within Singapore. The region is largely made up of residential towns, established industrial estates, educational and recreational uses. The variety of land-uses creates great opportunities for short-distance travel, which can generate demand for cycling. This also may generate a large variation of the bikeability level and should be useful for further planning of new cycling routes.

To assess the bikeability of existing cycling infrastructure in the study area, we used a road network obtained from Land Transport Authority Singapore (LTA, 2017), and integrated it with cycling routes. Overall, we considered three types of cycling infrastructure, including on-road bike paths, footpaths and separate cycling routes (involving cycling paths and park connector network -PCN) (see

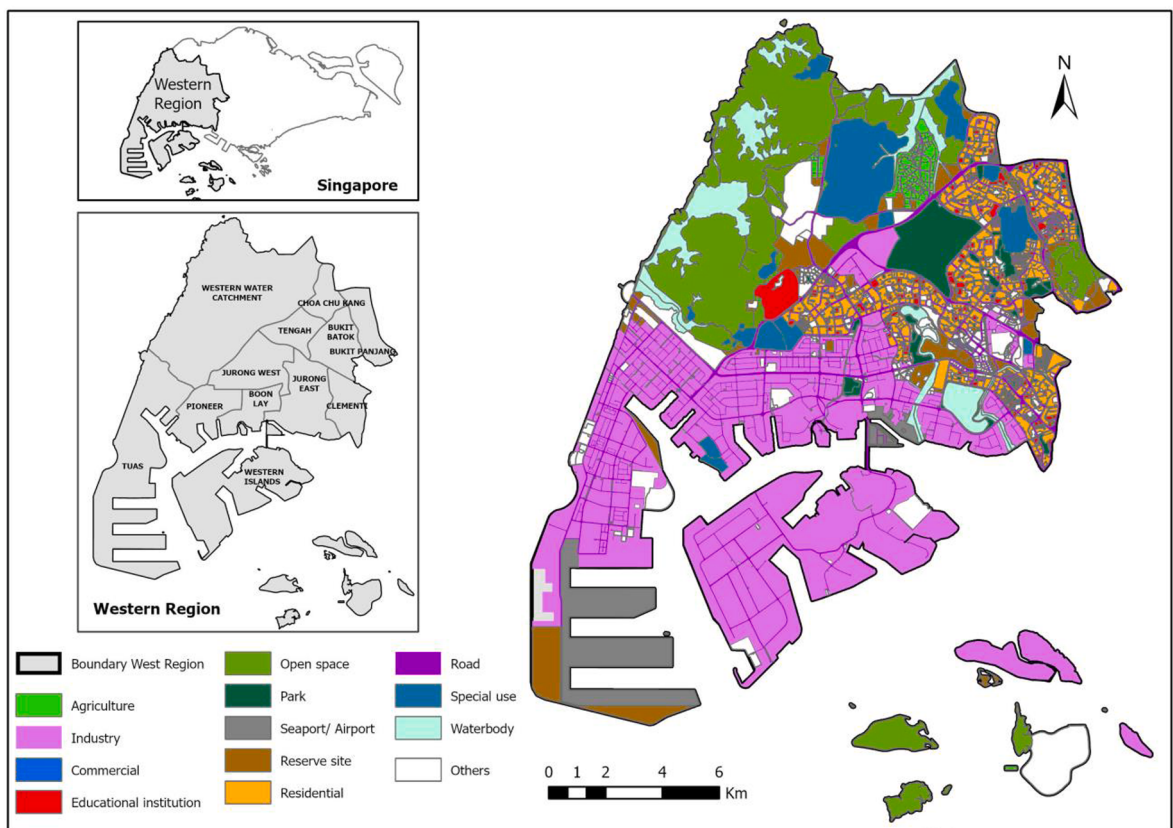


Fig. 2. Location of the study area and districts and land use maps within it.

Fig. 3). Since in most cases, air quality, amenities and physical attributes varied within each road and across roads, the roads were broken into segments based on road intersections. We disregarded the road segments that do not allow for cycling (e.g., on the highway, restricted access areas in the Western island). A total of 2331 road segments with the average segment length of 240 m (from 11.1 m to 630.2 m) were used for the evaluation of the bikeability index. Other spatial datasets collected in this study include PM_{2.5}, BC concentration, land use data, points of interest (POI), digital elevation model (DEM) and GSV images. The descriptive statistics of datasets and their respective sources are included in **Table 2**. The process to calculate each indicator score is described in detail in the following sections.

3.3. Calculation of sub-indices and Indicators

3.3.1. Air quality

3.3.1.1. PM_{2.5} and BC measurements. PM_{2.5} and BC mass concentrations were obtained during a mobile measurement campaign using bicycles in November 2019. Six routes of 7.0–17.5 km each were designed to cover many land-uses and different road categories (**Fig. 4**). PM_{2.5} and BC measurements were conducted at least two times per biking route on weekdays, from 7:30 am to 10:00 am, and 10:00 am to 12:30 pm to cover traffic peak and non-peak hours, respectively.

The portable devices that were deployed in this study included two sets of handheld particle counters (Particles Plus 8306, USA) and micro-Aethalometers (AE51, Aethlabs, USA). Particles Plus 8306 is a real-time particle counter that measures the particle number concentration in the range of 0.3–25 µm particles (#/m³) with a flow rate of 2.83 L per minute using a laser diode technology. The devices were factory-calibrated to meet ISO 21501-4 and JIS B9921 standards. The Particles Plus also reports PM_{2.5} mass concentration (µg/m³) with the default particle density and refractive index. To get reliable PM_{2.5} mass concentrations under local weather conditions, the two Particles Plus were pre-calibrated with a gravimetric sampler (MiniVol, Airmetrics, USA). Calibration steps of the Particles Plus are presented in section S1 of the Supplementary Information (SI). The final PM_{2.5} concentrations were obtained by multiplying the measured PM_{2.5} data obtained from the two devices by the corresponding calibration factors (i.e., 1.16 and 1.09) (Eq. (1) following). Moreover, meteorological variables, including air temperature (T) and relative humidity (RH), were also recorded using the Particles Plus units.

$$\text{Final PM}_{2.5} \text{ concentration}(\mu\text{g.m}^{-3}) = \text{Measured PM}_{2.5} \text{ concentration}(\mu\text{g.m}^{-3}) \times \text{CF} \quad (1)$$

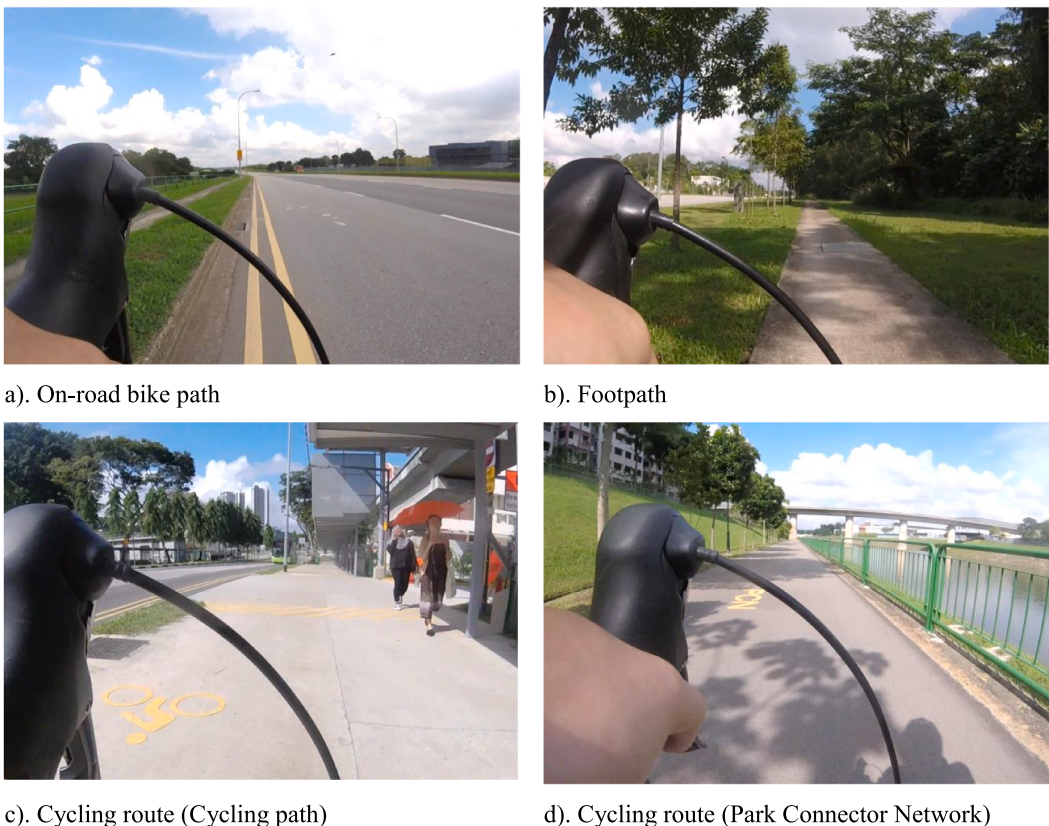


Fig. 3. Typical cycling infrastructure (Screenshot from video footage during measurement campaign).

Table 2

Descriptive statistics of the datasets and their sources.

Sub-index	Dataset	Description	Number of data	Unit	Data type	Data sources
Air quality	PM _{2.5} and BC concentrations	Cyclists' exposure to PM _{2.5} and BC	8368 (each pollutant)	µg/m ³	Point	On-site measurement (69 km cycling)
	Land use data	Distance to the closest rail line	2331	m	Polyline	(LTA, 2017)
		Distance to the closest highway, shore, airport/seaport	2331	m	Polygon	(LTA, 2017; URA, 2014)
		Area of the business, open area, parks, residential, waterbody land use (Buffer: 50 m, 100 m, 200 m, 300 m, 500 m, 750 m, 1000 m)	2331(each buffer)	m ²	Polygon	(URA, 2014)
		Number of intersections, bus stops (Buffer: 50 m, 100 m, 200 m, 300 m, 500 m, 750 m, 1000 m)	2331 (each buffer)	#	Points	(LTA, 2017, 2019a)
		Length of highways, roads (Buffer: 50 m, 100 m, 200 m, 300 m, 500 m, 750 m, 1000 m)	2331 (each buffer)	m	Polyline	(LTA, 2017)
		Population (Buffer: 500 m, 750 m, 1000 m)	2331 (each buffer)	#	Polygon	(MTI, 2016)
Accessibility	Points of interest	Leisure (entertainment, sports, nature, food, tourist attraction)	1509	#	Point	(Baidu Inc., 2019)
		Transport (airport, MRT station, bus stops)	858	#	Point	(Baidu Inc., 2019)
		Commercial (enterprise, financial industry)	7195	#	Point	(Baidu Inc., 2019)
Suitability	DEM dataset	Daily routine	2906	#	Point	(Baidu Inc., 2019)
	Road and cycling network	Slope of each road segment	—	—	Raster	(USGS, 2020)
Perceptibility	GSV images	Simuosity and bike route	2331	—	Polyline	(LTA, 2017, 2019b)
		Cyclists' perception of greenery, crowdedness, outdoor enclosure	18,516	#	Image	(Google Developers, 2018)

**Fig. 4.** Sampling routes.

where CF is the calibration factor.

Two micro-Aethalometers AE51 were used to quantify BC concentration by measuring the attenuation of light transmitted through airborne particles that are continuously collected onto a small Teflon-coated borosilicate glass fiber filter. The filter strips were

replaced frequently to minimize filter loading effects (all the optical attenuation ATN values were observed below 40). Before air sampling, the pump flow rates were calibrated automatically using a flowmeter (TSI 4100, USA) as the manufacturer's recommendation. The micro-Aethalometer was then set up with the flow rate of 100 mL min^{-1} during the sampling. Negative or constant values in the recorded data, which are caused by instrumental noise at high logging intervals or very low BC concentrations, were resolved by using the Optimized Noise reduction Averaging (ONA) algorithm tool (Hagler et al., 2011). We also checked the performance of the AE51 by collocating the two units with an Aethalometer AE33 (Magee Scientific, USA) over 24 h of measurement with a good agreement (The data are shown in Fig. S4).

Finally, a mobile phone GPS app (Sensor Play-IOS app) was used to track the movement of research assistants conducting the measurements. Particles Plus and micro-aethalometer AE51 were set to capture data with a 10 s basin, whereas the GPS receiver was programmed logging data with a time resolution of 1 s. All real-time monitoring equipment was placed in a bicycle basket, and inlets of air sampling tubing were kept within the breathing zone. All the PE measurements were conducted only during sunny periods with clear skies (in the morning and noon periods) to avoid misrepresentation of urban air pollution conditions due to the wet scavenging of aerosols which happened frequently in the afternoon and evening during the measurement month (i.e., November 2019). It should be noted that there is no significant difference in air quality levels between morning and evening traffic peak hours in Singapore (Tran et al., 2020a). The non-rainy sampling periods were also chosen to protect the measurement devices and their operational integrity and to avoid any measurement bias caused by high relative humidity.

3.3.1.2. Land-use regression models. Understanding the small-scale variations of $\text{PM}_{2.5}$ and BC in an urban area is crucial for accurate PE assessment. The cost of sampling equipment and the lack of availability of human resources often restrict large-scale monitoring campaigns with numerous simultaneous measurements of $\text{PM}_{2.5}$ and BC. Therefore, land-use regression (LUR) models, which provide an empirical approach to determine the spatial variability of air pollutant concentrations (Brauer et al., 2003; Briggs et al., 2000; Marshall et al., 2008), have been widely used in many exposure assessments studies (e.g., Minet et al., 2018a, 2018b; Van den Bossche et al., 2018; Van den Hove et al., 2019). Compared to LUR models built based on fixed measurements of air pollutants, those based on mobile monitoring do not only expand spatial coverage for data acquisition but also enlarge the sample size.

In this study, we developed $\text{PM}_{2.5}$ and BC LUR models using mobile measurements (i.e., cycling) based on the approach described by Minet et al. (2018a). There are three main steps involved in LUR models. First, for each road segment, we computed 10 land-use variables within buffers of sizes 50, 100, 200, 300, 500, 750 and 1000 m drawn around the segments. These variables include the area of the business, open area, parks, residential, and waterbody land uses; the number of intersections and bus stops; the length of highways and roads; and the population. Additionally, we calculated for each road segment its distance to the closest rail line, highway, shore, airport and seaport. Details are provided in Table 2 and in section S3 of the SI. Next, significant independent variables were selected on the basis of the adjusted R^2 values and the p-value of the linear regression between the variable and $\ln(\text{PM}_{2.5})$ or $\ln(\text{BC})$ to develop stepwise regression models. Finally, the models were evaluated with 100-fold cross-validation (details of the steps are described by Minet et al. (2018a)) to select the best models. Equation (2) describes the final LUR models.

$$\ln(\text{PM}_{2.5}\text{orBC}) = b_0 + \sum_i b_i * \text{variable}_i \quad (2)$$

where $\ln(\text{PM}_{2.5}$ or BC) is the natural logarithm of $\text{PM}_{2.5}$ or BC concentration; b_0 and b_i are fixed coefficients; variable_i is a land-use variable found significant.

For each segment of the study area, we calculated the land-use variables included in the LUR models and predicted the $\text{PM}_{2.5}$ and BC concentrations.

3.3.2. Accessibility, suitability and perceptibility

Our accessibility sub-index was calculated based on the density of possible cyclist destinations, which was described by the number of POIs along each road segment (Eqs. (3)–(6) following). A database of POIs was obtained from Baidu Map using an API interface in November 2019 (Baidu Inc., Beijing, China). The data consisted of four categories of facilities: leisure (entertainment, sports, nature, food, and tourist attractions), transport (airport, MRT stations, and bus stops), commercial locations (enterprise and financial industry), and daily routine as shown in Table 2.

$$\text{Leisure}_i = \sum \text{POI}_{\text{leisure}}_i \quad (3)$$

$$\text{Transport}_i = \sum \text{POI}_{\text{transport}}_i \quad (4)$$

$$\text{Commercial}_i = \sum \text{POI}_{\text{commercial}}_i \quad (5)$$

$$\text{Dailyroutine}_i = \sum \text{POI}_{\text{dailyroutine}}_i \quad (6)$$

where i indicates individual road segment in the road network.

For assessment of suitability, we considered three indicators to describe the cycling suitability of each road segment, including slope, sinuosity and bike route. The slope was produced upon the DEM dataset (USGS, 2020) and sinuosity was determined by calculating the ratio of the actual length of a road segment to the length between the initial and endpoint of the segment (i.e., based on

the segment coordinates) as shown in Eq. (7) (Su et al., 2019). The bike route captures on-road bike paths (assigned a score of 0), footpaths (a score of 0.5), separate cycling routes (including cycling paths and park connector network) (a score of 1.0) to consider the safety aspect of cycling on a relative scale. Cycling on-road and sharing space with motorized vehicles is more dangerous than cycling on footpaths and sharing space with pedestrians, whereas it is the safest to cycle on dedicated cycling routes. In comparison with Peter Furth's classification (Furth, 2014) on Level of Traffic Stress (LTS), "stand-alone paths" and "separated paths" are along with our cycling routes (cycling paths and park connector network) (illustrated in Fig. 3); his classification of "mixed traffic" is similar to our on-road bike paths. The LTS criteria for "bike lanes" as described in Peter Furth's work are not applicable to Singapore conditions where the narrow on-road bike paths (around 30–40 cm width) is as dangerous as mixed traffic conditions. Cycling on roads out of this narrow lane is not allowed by traffic rules in the country.

$$\text{Sinuosity}_i = \frac{\text{Length}_i}{\sqrt{(x_2 - x_1)^2 + (y_2 - y_1)^2}} \quad (7)$$

where sinuosity_i is the sinuosity value of road segment i ; Length_i is the length of road segment i ; (x_1, y_1) and (x_2, y_2) are the coordinates of the initial and endpoint of road segment i , respectively.

To calculate the perceptibility sub-index, we first downloaded GSV imagery on each road segment using GSV API. Four images (i.e., 0°, 90°, 180°, and 270°) at each location were downloaded to cover 360° horizontal surroundings as a view area reflecting eye-level equivalent cyclist experience. A total of 18,516 GSV images were collected. Next, we detected the targeted physical features in each image by performing an accurate semantic segmentation, which is a process that partitions a given image into multiple proportions and labels each pixel in the categories (described below) to which it belongs. A high accuracy segmentation model using a deep neural network, named SegNet and proposed by Badrinarayanan et al. (2017), was used in this study (Fig. 5). The architecture of SegNet consists of an encoder network, a decoder network followed by a pixel-wise classification layer. It is only convolutional without fully connected layers. After a training process with off-the-shelf image dataset called the Cambridge-driving Labeled Video Database (CamVid) (Brostow et al., 2008, 2009), the model initially divided the image into 12 classes (i.e., sky, building, pole, pavement, road, tree, sign symbol, fence, vehicle, pedestrian, cyclist, and road marking) with a training accuracy of 96.7%, and a validation accuracy of 79.6%. The CamVid dataset was selected for the training process due to the similarity of road structure in Singapore and in the UK. Representative results of segmentation are displayed in Fig. S3.

We calculated the number of pixels in each class in the segmentation imagery and deployed a method proposed by Zhou et al. (2019) to calculate the perceptibility for each road site. It is important to note that for this proposed method, many related factors such as street greenery and perceptions of safety were evaluated systematically (Zhou et al., 2019). The perceptibility is composed of three sub-indicators including greenery, crowdedness and outdoor enclosure. Greenery and crowdedness refer to the visibility of road vegetation and obstacles, respectively, which can influence cyclist psychological feelings. The outdoor enclosure was defined by the ratio of vertical elements (e.g., building, tree) to horizontal features (e.g., pavement, road) (Zhou et al., 2019). The appropriate outdoor enclosure can provide the cyclist with comfortable feeling (Jacobs and Appleyard, 1987). All the formulae and explanations of the

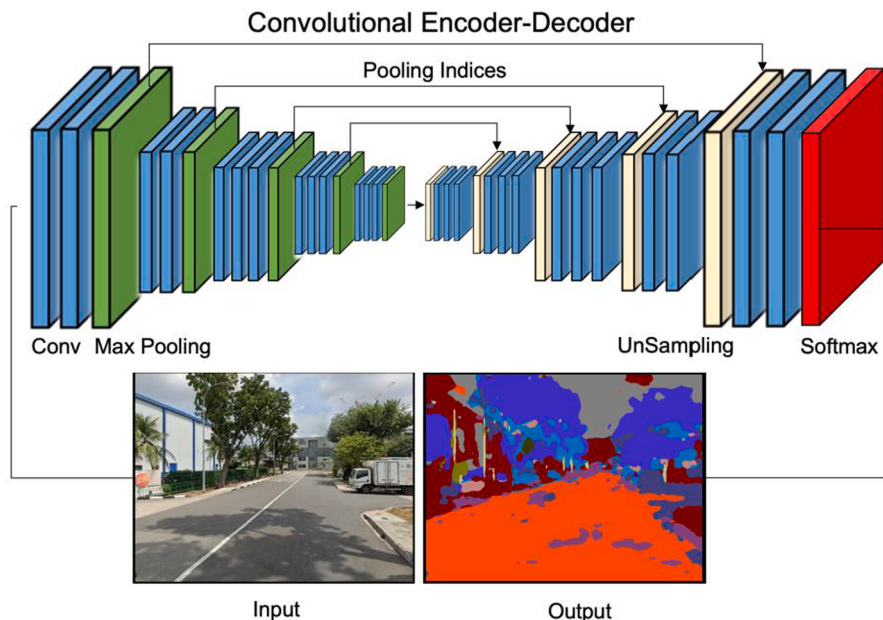


Fig. 5. The architecture of SegNet consists of an encoder network and a decoder network followed by a pixel-wise classification layer. It is an only convolutional architecture without fully connected layers.

three sub-indicators and the final perceptibility of road segment i are shown in Eqs. (8)–(10).

$$\text{Greenery}_i = \frac{\sum_1^4 T_n}{4 * \text{Sum}} \quad (8)$$

$$\text{Crowdedness}_i = \frac{\sum_1^4 C_n}{4 * \text{Sum}} \quad (9)$$

$$\text{Outdoor Enclosure}_i = \frac{\sum_1^4 B_n + \sum_1^4 T_n}{\sum_1^4 P_n + \sum_1^4 R_n + \sum_1^4 F_n} \quad (10)$$

where greenery_i, crowdedness_i, and outdoor enclosure_i represent greenery, crowdedness and outdoor enclosure values of road segment i; T_n, C_n, B_n, P_n, R_n, and F_n are the number of trees, obstacles (pedestrians, cyclists, and vehicles), buildings, pavement, roads, and fence pixels, respectively on image n of road segment i; n indicates individual GSV image (n = 1, 2, 3, 4 corresponds to a view of 0°, 90°, 180°, and 270° of the GSV image at each location). Sum is the total pixel number of all physical features on 4 images of the road segment i.

3.3.3. Composite bikeability index and cluster analysis

All 12 indicators were measured in different units with diverse value ranges (descriptive statistics of 12 indicators are shown in Table 3). Therefore, a normalization process was required to integrate such diverse criterion values into a single bikeability. The indicators were normalized using Eqs. (11) and (12).

$$\dot{I}_{ij} = \begin{cases} \frac{I_{ij} - \min I_{ij}}{\max I_{ij} - \min I_{ij}}, & \text{positive indicator.} \\ \frac{\max I_{ij} - I_{ij}}{\max I_{ij} - \min I_{ij}}, & \text{negative indicator.} \end{cases} \quad (11,12)$$

where I_{ij} is the value of indicator i for segment j; max I_{ij} and min I_{ij} are the maximum and minimum values of the indicator i for all segments. Positive indicators with greater values denote higher bikeability (i.e., greenery, bike routes and accessibility indicators), while negative indicators with lower values denote higher bikeability (i.e., crowdedness, slope, sinuosity and air quality indicators). The value of outdoor enclosure was classified into two ranges: (1) as a positive indicator if the values fell between min I_j and I_j*; (2) as a negative indicator if the values fell between I_j* and max I_j. I_j* = 1.6 was adopted as a recommended outdoor enclosure to provide a comfortable feeling for cyclists (Jacobs and Appleyard, 1987). After normalization, the score of each indicator ranged between 0 and 1. The higher the value of the score, the better the indicator.

To derive the bicycle-friendly level of road segments and integrate all 12 indicators, the Weighted Linear Combination model was used as Eqs. (13) and (14).

$$S_{kj} = \sum_{i=1}^n w_i \dot{I}_{ij} \quad (13)$$

$$B_j = \sum_{k=1}^4 w_k S_{kj} \quad (14)$$

where S_{kj} is the sub-index k of the segment j, w_i is the weighting of the indicator i, B_j is the overall bikeability value of the segment j and w_k is the weighting of sub-index k.

Both Global and Local Moran's I were used in this study. Global Moran's I (Moran, 1950) was deployed as a spatial autocorrelation

Table 3

Descriptive statistics of 12 indicators of the bikeability index (N = 2331).

Sub-index	Indicator	Maximum	Minimum	Mean	Standard deviation
Accessibility	PM _{2.5} (µg/m ³)	20.11	8.38	17.07	2.59
	BC (µg/m ³)	10.32	3.59	4.78	1.03
	Leisure (#)	25	0	1	4.23
Suitability	Transport (#)	4	0	1	0.82
	Commercial (#)	81	0	4	16.33
	Daily routine (#)	49	0	2	7.24
Perceptibility	Slope	15.06	0.00	5.37	2.48
	Sinuosity	4.80	1.00	1.48	0.56
	Bike route	1	0	0.53	0.20
	Greenery	0.55	0.02	0.19	0.06
	Crowdedness	0.49	0.14	0.29	0.06
	Outdoor enclosure	9.74	0.47	1.40	2.07

analysis to investigate the spatial disparities of bikeability on the road network. The value of global Moran's I index varies from -1 to 1 : “ 0 ” implies perfect spatial randomness; “ 1 ” means perfect positive spatial autocorrelation (high value or low values cluster together); and “ -1 ” suggests perfect dispersion (a checkerboard pattern). Global Moran's I quantifies only an overall measurement of spatial autocorrelation.

To identify local spatial cluster patterns and spatial outliers of the bikeability index and each sub-index, Local Moran's I index (Anselin, 1995) was further adopted. A high positive Local Moran's I value, including High-High (HH) cluster and Low-Low (LL) cluster, suggests a spatial cluster of the location. These clusters mean that the target segment and its neighbouring segments all have similarly high or low scores, respectively. In contrast, a possible spatial outlier is indicated via a high negative local Moran's I value to represent the noticeable difference of one location and its surroundings. High-Low (HL) outliers and Low-High (LH) outliers belong to spatial outliers, expressing a high score adjacent with low scores and a low score adjacent with high scores, respectively. For example, if there are HH (or LL) clusters of bikeability index in the study area, the road segments in these clusters all have high (or low) bikeability levels and so do the neighbouring roads. Transportation authorities and policy makers should pay attention to roads in LL clusters as well as HL and LH outliers to investigate the reason as to why there are spatial correlations between those road segments, and should devise strategic plans to improve the cycling infrastructure (Zhang et al., 2019).

4. Results and discussion

4.1. Air quality

Using PM_{2.5} and BC data collected during cycling, we generated the cyclists' PE while travelling on the road network. Table 4 presents the results of the two selected LUR models: ln(PM_{2.5}) based on four independent variables (including temperature, relative humidity, population within 1000 m, park area within 100 m) and ln(BC) based on four independent variables (temperature, relative humidity, business area within 500 m, and number of bus stop within 100 m). The adjusted R² for PM_{2.5} and BC models are 0.55 and 0.49, respectively. The values fall within the range of R² presented in the literature (i.e., 0.23–0.85 for PM_{2.5} and 0.28–0.86 for BC), based on short-term mobile monitoring (Hankey et al., 2017; Minet et al., 2017, 2018a, 2018b; Van den Bossche et al., 2018; Van den Hove et al., 2019).

Temperature and relative humidity are negatively associated with PM_{2.5} and BC in both selected LUR models, which are in agreement with previous studies (Hatzopoulou et al., 2013; Yang et al., 2018). The negative effects of temperature can be explained by different patterns of PM concentrations and temperature in the morning and noon time periods. During the morning peak hours (the temperature was lower), the shallow boundary layer accumulates air pollutants due to poor dispersion, resulting in elevated concentrations of PM_{2.5} and BC. In contrast, during the non-peak hours, there are lower emissions of PM_{2.5} and BC, and the deep boundary layer with strong vertical mixing of air further reduces their concentrations. As for the relative humidity, when its value is high, airborne particles tend to grow in size due to absorption of moisture and fall out, thereby reducing their concentration in the air, leading to a negative association between relative humidity and particulate concentrations (Liu et al., 2011). The other two important predictors of PM_{2.5} are human population within 1000 m and the presence of public parks within 100 m, which exhibit negative signs in the regression. We can explain the negative association between population and PM_{2.5} by the land use characteristics of WR, which include a large portion of dense industrial estates (i.e., low population density). These industrial areas had higher PM_{2.5} concentrations compared to the residential town (i.e., high population density) because of the movement of heavy duty vehicles. On the other hand, business areas within 500 m and the number of bus stops within 100 m appear in the BC model with positive signs, which is consistent with previous LUR studies (Minet et al., 2018a, 2018b).

Fig. 6 presents the spatial variations of average PM_{2.5} and BC concentrations derived from the LUR models. The average levels of PM_{2.5} and BC were $17.1 \pm 2.6 \mu\text{g}/\text{m}^3$ and $4.8 \pm 1.0 \mu\text{g}/\text{m}^3$, respectively. In general, cyclists' exposure to PM is relatively high near strong emission sources such as industrial areas and power plants, or major roads with a high traffic volume and a high number of bus stops (mostly in Tuas, Pioneer, Boonlay, Jurong East Districts) but lower in areas that are closer to public parks/green areas (e.g., in Bukit Batok, Choa Chu Kang Districts). These spatial disparities of PM concentration levels observed on road segments in this study are different from general observations made from fixed air quality monitoring stations which report small variations across regions in Singapore (Gall et al., 2015). Our results, therefore, corroborate findings from other studies (Adams et al., 2001; Kaur et al., 2007; Tran et al., 2020a), which emphasized the need for assessing the PE of urban dwellers to PM as part of air quality improvement efforts. High

Table 4
LUR models of PM_{2.5} and BC.

Variables	ln(PM _{2.5})		ln(BC)	
	Standardized Coefficients	p-value	Standardized Coefficients	p-value
Temperature	-6.25E-01	1.43E-10	-8.23E-01	1.81E-11
Relative humidity	-3.41E-01	1.72E-04	-5.73E-01	7.46E-07
Population within 1000 m	-4.56E-01	1.16E-14	-	-
Park area within 100 m	-2.09E-01	6.40E-05	-	-
Business area within 500 m	-	-	2.37E-01	5.54E-04
Number of bus stop within 100 m	-	-	1.58E-01	4.27E-03
Adjusted R ²	0.551		0.486	

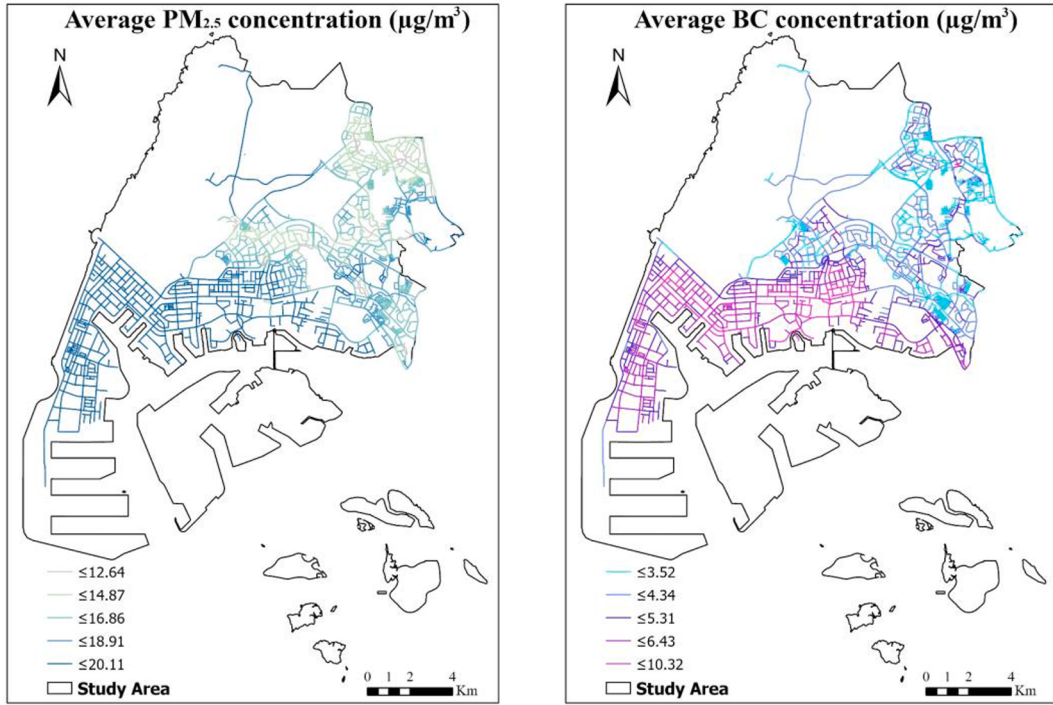


Fig. 6. Average $\text{PM}_{2.5}$ and BC concentrations on each road segment derived from the LUR models.

ratios of BC to $\text{PM}_{2.5}$ (≈ 0.29 on average) indicate a significant contribution of fossil fuel combustion (e.g., vehicle exhaust, especially from diesel vehicles), which are comparable to values reported in other studies in Singapore (Adam et al., 2020; Tan et al., 2017; Tran et al., 2020a).

$\text{PM}_{2.5}$ and BC data were then normalized, and an average score of the air quality sub-index was determined, as displayed in Fig. 7a. The higher the score, the lower the cyclist exposure to $\text{PM}_{2.5}$ and BC concentrations. The results of the cluster and outlier analysis using Anselin Local Moran's I are shown in Fig. S4. Based on the level of similarity in land use patterns and close proximities of precincts, the 11 districts in WR were grouped into four areas: East (Jurong West, Jurong East, Clementi, and Bukit Batok districts), North (Bukit Panjang, Choa Chu Kang, and Tengah districts), South (Tuas, Boon Lay and Pioneer districts) and West (Western Water Catchment). The score of air quality is lower in roads across the Southern areas within the WR of Singapore than in other neighbourhoods in the region. This may be because of high emissions of PM from Singapore's heavy industries located over there, mainly the petrochemical industry present in this area, as well as the frequent movement of trucks/high duty vehicles supplying goods and services to industries. The distribution of the air quality sub-index is shown together with other sub-indices of the bikeability by box plots in Fig. 8. The lower quartile of the air quality sub-index comprises a larger proportion, suggesting lower air quality (i.e., poor air quality) in many segments in the network.

4.2. Accessibility, suitability and perceptibility

The spatial pattern of the accessibility sub-index is shown in Fig. 7b; details on the four indicators are shown in Fig. S5. In general, the accessibility sub-index presents a widely dispersed spatial distribution due to multiple land-use urban developments because of space constraints in Singapore. For example, segments within Tuas district exhibit lower accessibility due to specific land uses (e.g., industrialization) while other neighbourhoods have mixed land-use patterns (Fig. 2). The presence of segments with a very high number of POIs in the study area has lowered the normalized score of the accessibility sub-index (mean = 0.1, shown in Fig. 8).

Fig. 7c displays the spatial pattern of the suitability sub-index, and Fig. S6 shows the corresponding indicators at the segment level. Road segments within Jurong West and Jurong East districts were observed to have higher suitability scores than roads in other neighbourhoods due to the presence of many cycling paths and PCN. In the Southern area (e.g., Tuas district), roads present relatively high suitability scores, which can be explained by its topography, having flattened industrial areas and land reclamation areas in this region. The reclaimed lands are usually flatter, which act in favor of the score of the slope indicator, and the roads in this area are straighter, resulting in a high score for the sinuosity indicator.

Spatial patterns of perceptibility and its indicators are shown in Fig. 7d and Fig. S7, respectively. The distribution of estimated perceptibility varies spatially across different locations and road segments. Roads in the Northern areas (e.g., Bukit Batok, Bukit Pan Jang, Choa Chu Kang districts) generally show a higher degree of greenery than in the southern areas. It is obvious that the degree of crowdedness is higher (i.e., the score is lower) in residential areas (mostly in the Northern and Eastern areas) than other parts of the

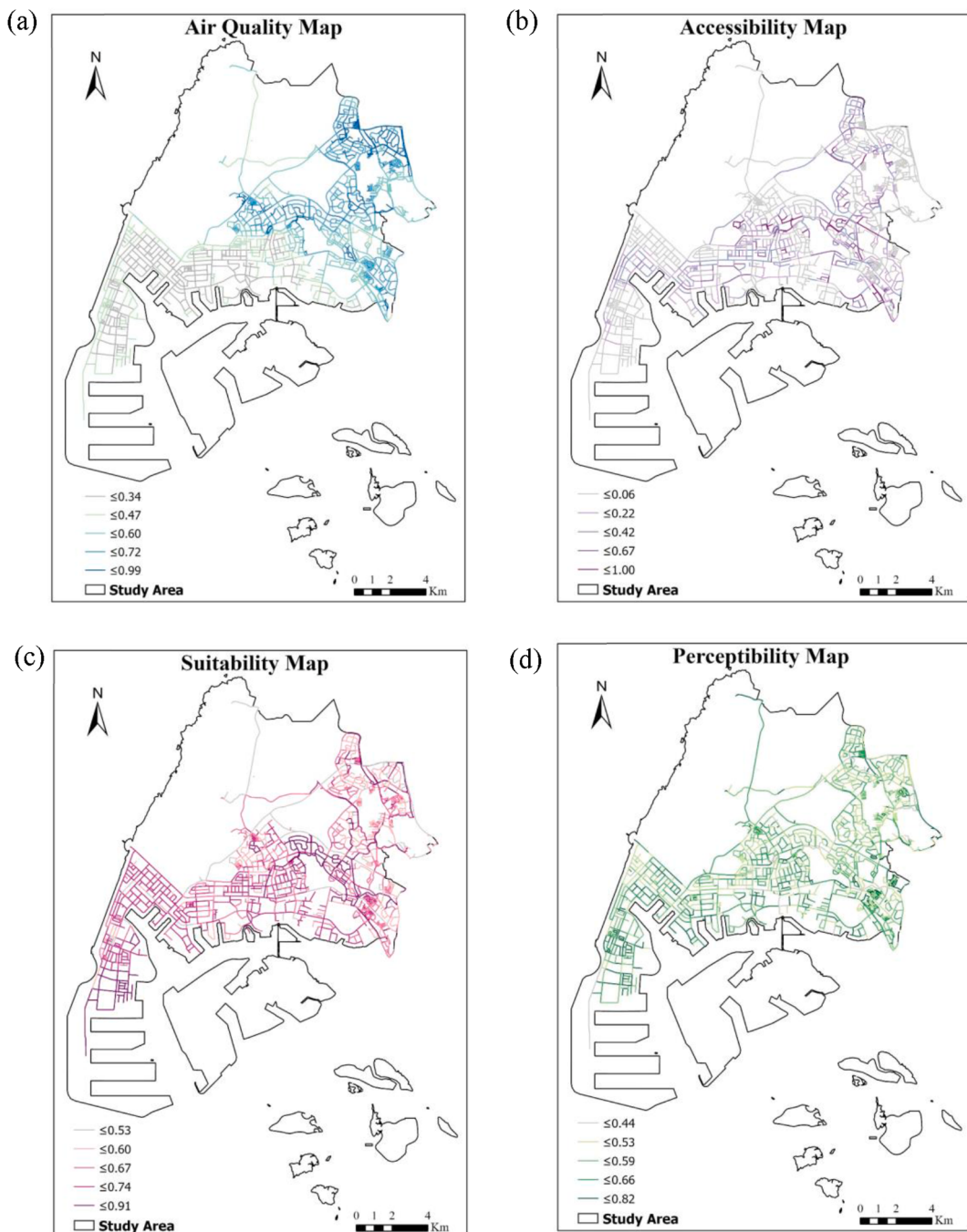


Fig. 7. Spatial patterns of four sub-indices: (a) Air quality, (b) Accessibility, (c) Suitability and (d) Perceptibility at segment levels within the Western Region.

WR. This may be because of the presence of many obstacles (e.g., cyclists, pedestrians, and cars) in the residential areas. Most road segments have outdoor enclosure values close to the recommended value to provide a comfortable feeling for cyclists (i.e., 1.6) (see Fig. S7).

4.3. Bikeability map and sensitivity analysis

4.3.1. The effects of air quality sub-index on bikeability

The effects of air quality on bikeability were evaluated by varying its weight from 0%, 12.5% to 25% (named as A0, A12.5 and A25

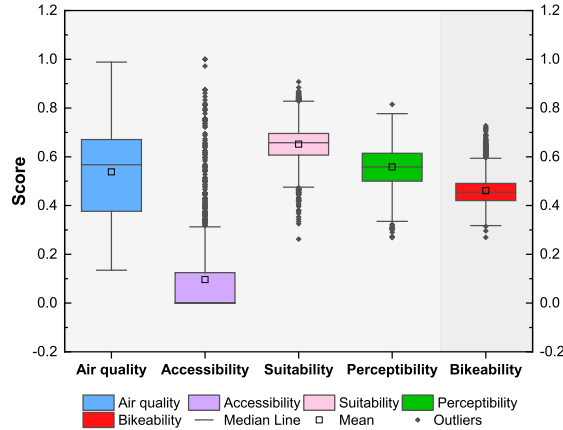


Fig. 8. Box plots for the integrated bikeability index and four sub-indices. (Bikeability was calculated with the equal contributions of each sub-index).

cases), and all other three other sub-indices (accessibility, suitability and perceptibility) have the same weights of 33.3%, 29.2% and 25%, respectively. The remaining weights of 25% for each sub-index (A25) were assigned based on the findings that in the Singapore context the selected indicators were all found to be important for cyclists (Koh and Wong, 2013, 2015; Meng et al., 2014). The same weights were also applied in some previous bikeability index calculation studies (Krenn et al., 2015; Winters et al., 2013). The moderate contribution of air quality (12.5%, A12.5) was added for comparison purposes.

When applying the A25 case to the study area in Singapore, the results show that about 19% of the road segments have low scores of ≤ 0.41 . Only 5% of road segments displayed high scores in most of 12 indicators, and the final score of bikeability ranges between 0.58 and 0.73. High score road segments are located near residential areas/parks/open spaces, on separate cycling paths, while low score road segments are usually characteristic of major roads/near industrial areas. In addition, most of the road segments (about 76%) are found with medium scores from 0.41 to 0.58. Among them, about 19% of the road segments have a higher score of air quality and perceptibility, but a lower score of accessibility and suitability; 7% of the road segments have a lower score of air quality and perceptibility, but a higher score of suitability. Data within the boxplot for the bikeability are symmetrically distributed around the mean value (Fig. 8), suggesting that the study area has an even distribution of segments with high and low scores for bikeability.

Fig. 9 illustrates the histograms of bikeability scores for the three cases A0, A12.5 and A25. By varying the contribution of air quality from 0% to 12.5% and 25%, significant changes were observed across four areas in terms of bikeability scores. Specifically, the scores increased in the Eastern, Northern and Western areas, but decreased in the Southern area. The bikeability index in 114 road segments in the East (or 163 road segments in the North) has increased by about 0.06–0.08 and 0.1–0.16 score between A0 – A12.5 and A0 – A25, respectively. On the other hand, the decrease of 0.08–0.04 score in 208 road segments in Southern areas was observed between A0-A25. The Western part of the study area has few road infrastructures despite being big and can therefore be disregarded. The decremental trend of bikeability scores in the South can be explained by its widespread presence of high exhaust emissions from heavy industry and the movement of a large fleet of trucks/high duty vehicles over there. These pollution sources resulted in negative effects of air quality sub-index on bikeability. In contrast, the presence of large environmental-friendly cycling infrastructures (e.g.,

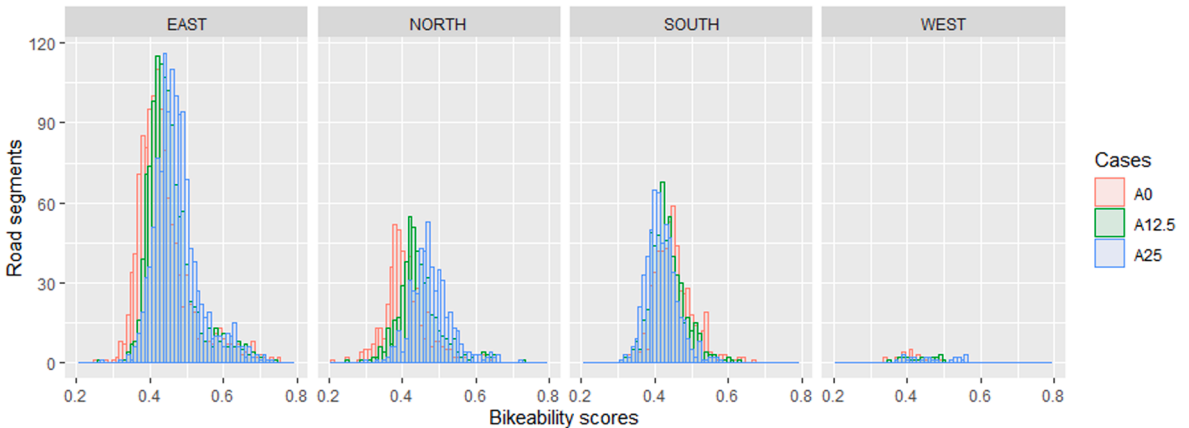


Fig. 9. Histograms of bikeability scores for the three cases A0 (0% weighting of air quality), A12.5 (12.5% weighting of air quality) and A25 (25% weighting of air quality).

park connector network) and green parks in the Eastern and Northern areas can explain the positive impacts of air quality sub-index across the three cases. In addition, the results of one-way analysis of variance (ANOVA) test with a p-value < 0.0001 between bikeability index in A25, A12.5 and A0 cases have confirmed the significant difference of the three datasets.

The differences of bikeability index and cluster analysis in spatial patterns between A25 and A0 cases are shown in Fig. 10a, c and Fig. 10b, d, respectively, whereas the A12.5 case is shown in Fig. S8. The results of global Moran's I (Moran's I index = 0.289, 0.139 and 0.150 for A25, A12.5 and A0, respectively, $p < 0.05$) reveal the existence of potential spatial patterns of the bikeability index in the study area. In particular, there are low levels (LL clusters) in the South (i.e., Tuas, Pioneer, Boonlay districts) and high levels (HH clusters) in the North (e.g., Choa Chu Kang district) in the bikeability map of the A25 case. In contrast, an opposite trend in spatial

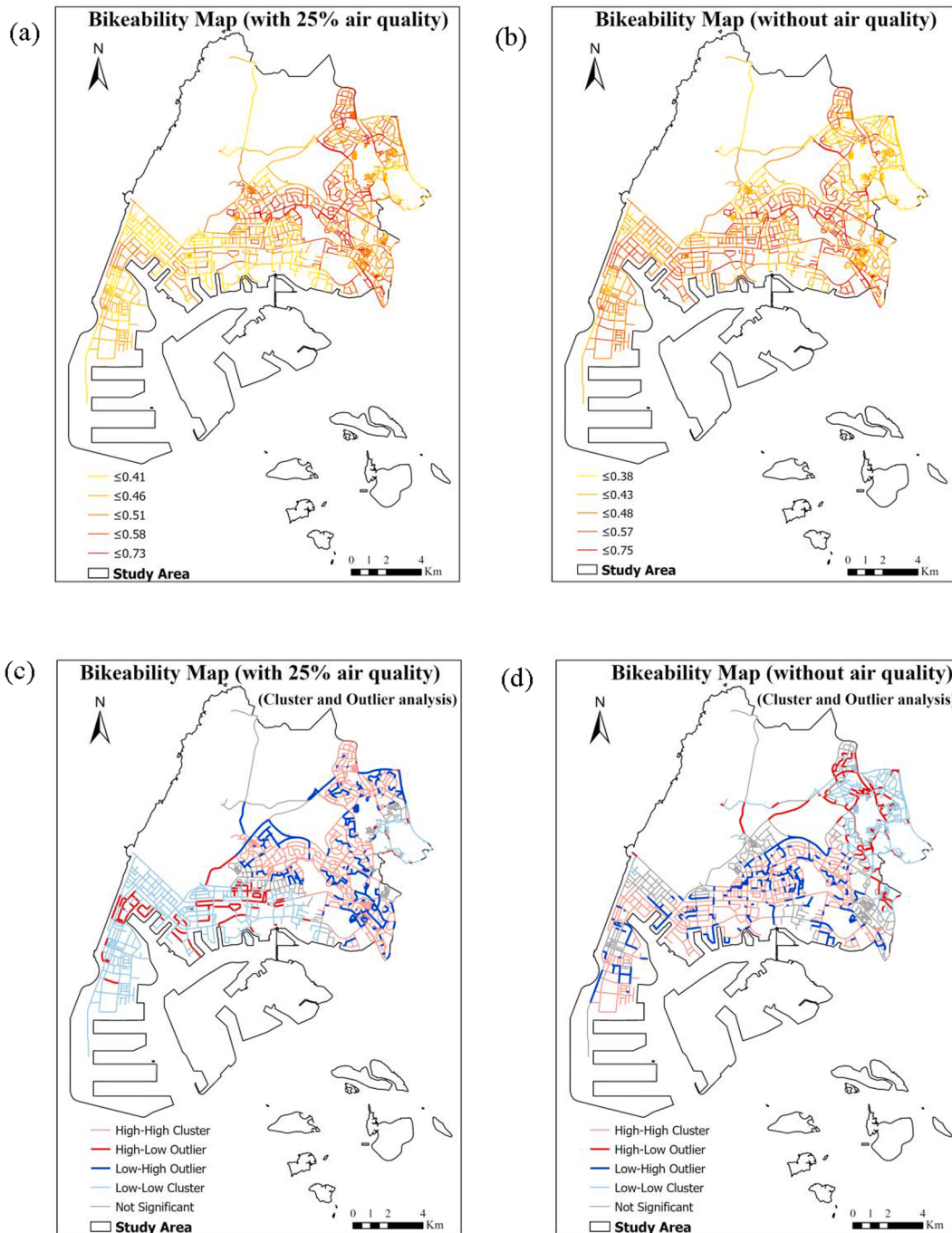


Fig. 10. Spatial patterns the bikeability index: (a) with air quality (A25 case); (b) without Air quality (A0 case) and (c, d) cluster and outlier analyses at each segment level within the Western Region.

distributions was observed for the A0 bikeability map (Fig. 10b and d). A significant discrepancy in the spatial pattern and cluster analysis was still observed between A12.5 and A0 cases (Fig. S8).

4.3.2. Sensitivity analysis

Sensitivity analysis was conducted to check the significance of air quality sub-index by exploring two additional scenarios. In total, three cases of air quality weighting (A0, A12.5 and A25 cases) were analyzed and integrated into three existing bikeability indices in literature with the following three scenarios:

Scenario 1: Balanced weights, proposed by Krenn et al. (2015) and Winters et al. (2013), are given as explained in Section 4.4.1. above.

Scenario 2: Suitability perspective was six times more important than perceptibility and accessibility, proposed by Lin and Wei (2018).

Scenario 3: Accessibility and suitability were two times more important than perceptibility, proposed by Porter et al. (2019).

For all scenarios, the inter-correlated ratios of the remaining three sub-indices were kept unchanged as in the original bikeability indices when air quality is added. We used a flexible weighting scheme to score and combine indicators, which enables users elsewhere to consider their local preferences and conditions. Table S4 describes detailed weights of all four sub-indices for all scenarios, which in turn need to be applied to the same WR study area. The p-values < 0.0001 were found for all cases from ANOVA analysis of bikeability index in the three scenarios, except p-values < 0.05 for 2 cases (between A0, A12.5 and A12.5, A25) in scenario 2. In general, the differences in all bikeability datasets are statistically significant.

For the study area, the results of sensitivity analysis are shown in Fig. 11 depicting the changes of cluster patterns when varying the weights of the air quality sub-index. Across all scenarios, the same trend of shifting cluster and outlier patterns (HH-High High cluster, LL-Low Low cluster, HL-High Low outlier, LH-Low High outlier and Non-not significant) was found, in which all non-segments increased from A0 to A12.5 and decreased from A12.5 to A25, whereas the HH cluster followed the opposite trend. The latter with the decrease/increase from A12.5 to A25 is more significant than the former with the increase/decrease from A0 to A12.5. Whereas, the remaining three clusters LL, LH and HL did not vary significantly. As we can see from Fig. 11, the increased number of HH clusters indicates that the existence of favorable air quality in those clusters has increased the bikeability index.

Similar results were observed for scenarios 1 and 3, where the number of all clusters and outliers were similar between A0 and A12.5 and varied significantly in A25. There is a significant decrease of Non-segments (from 33% to 18%, and 36% to 12%, respectively) and an increase of HH clusters (from 24% to 33%, and 21% to 31%, respectively) while increasing the weight of air quality from 0% to 25%. Whereas in scenario 2, the opposite trend was observed in which a similar number of all clusters and outliers occurred between A0 and A25; and varied significantly in A12.5. This can be explained by the complex interactions between sub-indices, characterized by their weighting, that influenced the impact of air quality on bikeability.

In general, based on the change of Non and HH cluster percentages from 10% to 20 % (as well as p-value < 0.0001), we can conclude that the bikeability/cyclability index has captured the cyclists' exposures to air pollution in the A25 case (with 25% air quality contribution) sufficiently. However, even the percentages of all clusters and outliers do not change significantly in the A12.5 case; the spatial distribution has shown the swapping between these clusters, e.g., from Non to HL, HL to LH and vice versa, etc. (see Fig. 10 (a,c) and Fig. S8). Together with p-value < 0.05 for all cases from the sensitivity analysis, it appears that the bikeability/cyclability index has captured the cyclists' exposures to air pollution in A12.5 (with 12.5% air quality contribution). This conclusion is based on the study area in Singapore only, which may vary while applying the proposed framework to other local conditions or other cities.

5. Limitations

This pilot study has some limitations. Firstly, the assessment of crowdedness indicator mainly depends on the GSV imagery detection, but street images in GoogleMaps database might be collected at various periods of the day and may not be representative across the study area. Therefore, future research should consider focusing on on-site observations and/or other sources of data to validate this study approach. Secondly, the distribution of the accessibility sub-index is skewed in the lower range of normalized scores (0.0–0.15) due to the consideration of the number of POIs as the key criterion in the calculation. The assessment of accessibility could be improved by including more indicators such as entropy index, intersection density, and road networks (Lin and Wei, 2018; Su et al., 2019).

Thirdly, the inter-correlation among individual indicators was not considered in this study, which motivates a further study to focus more on the individual contribution of each sub-index in a comprehensive bikeability. We only considered three levels of weights for air-quality, but other weighting methods (e.g., Delphi method) can also be explored. Furthermore, other environmental factors (e.g. noise pollution, night lighting), social factors (e.g. crime, social norm, co-participation in cycling) can be included to develop a comprehensive sustainable bikeability index. Lastly, it is also observed that the bikeability varies greatly across segments. Mapping the bikeability variations will provide useful references for transport planners to explore improvements in cycling infrastructure. More comprehensive studies building on the concept of bikeability developed in this study are warranted in other cities within the SEA or elsewhere to evaluate specific interventions, or to explore policy prescriptions.

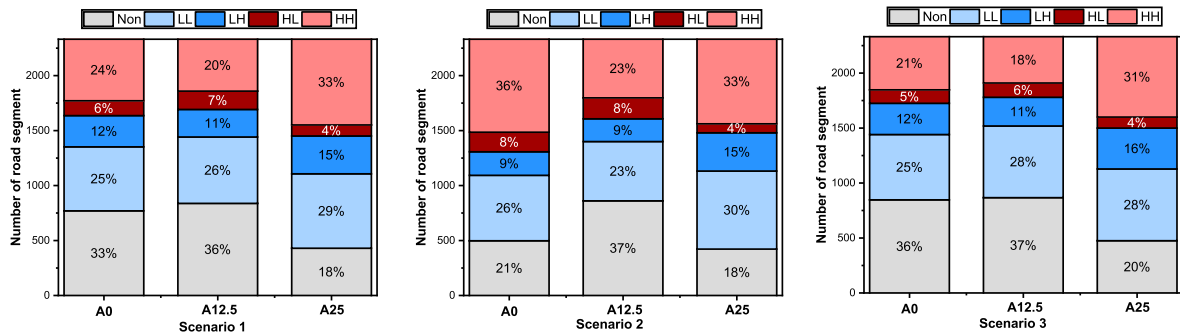


Fig. 11. Changes of cluster and outlier patterns while varying the weights of air quality sub-index in three scenarios. Non-not significant, LL-Low Low cluster, LH-Low High outlier, HL-High Low outlier and HH-High High cluster.

6. Conclusions

Despite its strong influence on cycling behavior, cyclists' personal exposure (PE) to TRAP has been often overlooked in current literature. Herein, we proposed a new bikeability framework by taking into consideration cyclists' PE to TRAP in conjunction with the other three sub-indices that are already in existence: accessibility, suitability and perceptibility. The comprehensive assessment of bikeability/cycling index with consideration of cyclists' PE to TRAP is useful to develop sustainable cycling infrastructure. In particular, our bikeability index with emphasis on cyclists' PE to PM_{2.5} and BC on each road segment derived from LUR models differs from existing cycling indices, which consider only qualitative questionnaire on air quality indicators regarding PE to air pollutants, or quantitative PM data obtained from fixed air quality monitoring stations.

This is the first-of-its-kind study that quantifies cyclists' PE to PM_{2.5} and BC on large scale road networks in the SEA region based on the integration of open-source data (such as land use map, road network, GSV imagery, POIs and DEM datasets), advanced SegNet deep neural network, and GIS spatial analysis. With this improved methodology, the data collection process is more efficient and less time-consuming compared to past studies, and more importantly the subjective assessment of bikeability is eliminated. In addition, cyclists' perspectives (e.g., perception on crowdedness, greenery and outdoor enclosure) were assessed through available GSV imagery in GoogleMaps database, which was processed using available SegNet. The bikeability framework we designed relies on widely available spatially-resolved data, and thus facilitates its widespread implementation.

Urban and transport planners and environmental policymakers can make use of the newly developed bikeability index objectively, and design cycling infrastructure accordingly in a comprehensive manner. We believe that the new concept of bikeability developed in this work can also be explored in other countries under different air pollution exposure scenarios and physical environments. To illustrate the application of the bikeability framework, we used Singapore as a testbed in this study. The study outcomes indicate that road segments within Tuas, Pioneer and Boonlay districts have higher suitability, but present moderate perceptibility and much lower accessibility and air quality, leading to a lower overall bikeability score compared to other regions. Therefore, to enhance cycling mobility, air quality, green spaces and multiple land-use patterns should be improved in those areas with low bikeability scores. The spatial patterns, clusters and outlier analyses have shown significantly different results when the bikeability index does not include the air quality component compared to the case with air quality. In other words, this study has demonstrated the importance of considering cyclists' exposure to airborne particles in transport microenvironments. Further sensitivity analysis has shown that with 25% weighting of air quality, the change of HH cluster numbers provides sufficient evidence to conclude that the bikeability/cyclability index has captured the cyclists' exposures to PM satisfactorily. 12.5% weighting of air quality can also lead to the same conclusion, but we suggest the 25% weighting of air quality in countries/regions with PE to high PM levels.

7. Practical implications

In this study, we generally observed elevated concentrations of PM_{2.5} and BC near industrial areas and major roads, and high ratios of BC to PM_{2.5} indicating a significant contribution of fossil fuel combustion to cyclists' PE to TRAP, especially from diesel vehicles. Therefore, in transport microenvironments such as the ones encountered in this study, it is important to improve near road air quality so that the bikeability score can be high by phasing out diesel-powered internal combustion engines or replacing them by vehicles using clean and green fuels or facilitating more public transport. Alternatively, minor shifts in the cycling network may reduce cyclists' exposure to PM, for example, moving cyclists away from strong air pollution emission sources with strategic locations of bicycle infrastructure on low-traffic roads. Cyclists could also be advised to avoid travelling during traffic peak hours to protect their health.

CRediT authorship contribution statement

Phuong T.M. Tran: Conceptualization, Data curation, Formal analysis, Methodology, Visualization, Writing - original draft. **Mushu Zhao:** Conceptualization, Data curation, Formal analysis, Visualization. **Kohei Yamamoto:** Conceptualization, Formal analysis. **Laura Minet:** Methodology, Writing - review & editing. **Teron Nguyen:** Data curation, Formal analysis, Writing - original

draft. **Rajasekhar Balasubramanian:** Supervision, Writing - review & editing.

Acknowledgements

This research was financially supported by the National Research Foundation (NRF), the Prime Minister's Office, Singapore, under its Campus for Research Excellence and Technological Enterprise (CREATE) program (R-706-002-101-281) and also by the National University of Singapore (R-302-000-195-133 & R-302-000-236-114). Technical help provided by Particle Plus (USA) in support of our study is gratefully acknowledged. We would like to acknowledge the editor and anonymous reviewers for their constructive feedback and valuable comments on the manuscript.

Appendix A. Supplementary material

Supplementary data to this article can be found online at <https://doi.org/10.1016/j.trd.2020.102563>.

References

- Adam, M.G., Chiang, A.W.J., Balasubramanian, R., 2020. Insights into characteristics of light absorbing carbonaceous aerosols over an urban location in southeast Asia. *Environ. Pollut.* 257, 113425.
- Adams, H., Nieuwenhuijsen, M., Colvile, R., McMullen, M., Khandelwal, P., 2001. Fine particle (Pm2. 5) personal exposure levels in transport microenvironments, London, UK. *Sci. Total Environ.* 279, 29–44.
- Aldred, R., 2019. Built environment interventions to increase active travel: a critical review and discussion. *Curr. Environ. Health Rep.* 6, 309–315.
- Andersson, A., Hiselius, L.W., Adell, E., 2018. Promoting sustainable travel behaviour through the use of smartphone applications: a review and development of a conceptual model. *Travel Behav. Soc.* 11, 52–61.
- Andreae, M., Gelencsér, A., 2006. Black carbon or brown carbon? The nature of light-absorbing carbonaceous aerosols. *Atmos. Chem. Phys.* 6, 3131–3148.
- Anowar, S., Eluru, N., Hatzopoulou, M., 2017. Quantifying the value of a clean ride: how far would you bicycle to avoid exposure to traffic-related air pollution? *Transp. Res. Part A: Policy Pract.* 105, 66–78.
- Anselin, L., 1995. Local indicators of spatial association—Lisa. *Geogr. Anal.* 27, 93–115.
- ASEAN, 2020. Association of Southeast Asian Nations, <https://asean.org/>, Last Access: 5 July 2020.
- Badrinarayanan, V., Kendall, A., Cipolla, R., 2017. Segnet: a deep convolutional encoder-decoder architecture for image segmentation. *IEEE Trans. Pattern Anal. Mach. Intell.* 39, 2481–2495.
- Baidu Inc, 2019. Point of Interest. Baidu Inc., Beijing, China.
- Berger, M., Dörzrapf, L., 2018. Sensing comfort in bicycling in addition to travel data. *Transp. Res. Procedia* 32, 524–534.
- Börjesson, M., Eliasson, J., 2012. The value of time and external benefits in bicycle appraisal. *Transp. Res. Part A: Policy Pract.* 46, 673–683.
- Brauer, M., Hoek, G., van Vliet, P., Meliefste, K., Fischer, P., Gehring, U., Heinrich, J., Cyrys, J., Bellander, T., Lewne, M., 2003. Estimating long-term average particulate air pollution concentrations: application of traffic indicators and geographic information systems. *Epidemiology* 228–239.
- Brauer, M., Freedman, G., Frostad, J., Van Donkelaar, A., Martin, R.V., Dentener, F., Dingenen, R.V., Estep, K., Amini, H., Apte, J.S., 2016. Ambient air pollution exposure estimation for the global burden of disease 2013. *Environ. Sci. Technol.* 50, 79–88.
- Briggs, D.J., de Hoogh, C., Gulliver, J., Wills, J., Elliott, P., Kingham, S., Smallbone, K., 2000. A regression-based method for mapping traffic-related air pollution: application and testing in four contrasting urban environments. *Sci. Total Environ.* 253, 151–167.
- Brostow, G.J., Shotton, J., Fauqueur, J., Cipolla, R., 2008. European Conference on Computer Vision. Springer, pp. 44–57.
- Brostow, G.J., Fauqueur, J., Cipolla, R., 2009. Semantic object classes in video: a high-definition ground truth database. *Pattern Recogn. Lett.* 30, 88–97.
- Day, K., 2016. Built environmental correlates of physical activity in china: a review. *Prevent. Med. Rep.* 3, 303–316.
- Department of Statistics Singapore, 2020. Geographic Distribution, <https://www.singstat.gov.sg/find-data/search-by-theme/population/geographic-distribution/latest-data>, Last Access: 24 April 2020.
- Furth, P.G., 2020 Level of Traffic Traffic Stress Criteria Criteria. <http://www.northeastern.edu/peter.furth/wp-content/uploads/2014/05/LTS-Tables1.pdf>, Last Access: 24 July 2020.
- Gall, E.T., Chen, A., Chang, V.W.-C., Nazaroff, W.W., 2015. Exposure to particulate matter and ozone of outdoor origin in Singapore. *Build. Environ.* 93, 3–13.
- Gholamiamal, A., Matisziw, T.C., 2019. Modeling bikeability of urban systems. *Geogr. Anal.* 51, 73–89.
- Google Developers, 2018. Gsv Api.
- Gu, P., Han, Z., Cao, Z., Chen, Y., Jiang, Y., 2018. Using open source data to measure street walkability and bikeability in China: A case of four cities. *Transp. Res. Rec.* 2672, 63–75.
- Hagler, G.S., Yelverton, T.L., Vedantham, R., Hansen, A.D., Turner, J.R., 2011. Post-processing method to reduce noise while preserving high time resolution in aethalometer real-time black carbon data. *Aerosol Air Qual. Res.* 11, 539–546.
- Handy, S., Cao, X., Mokhtarian, P.L., 2006. Self-selection in the relationship between the built environment and walking: empirical evidence from northern California. *J. Am. Plan. Assoc.* 72, 55–74.
- Hankey, S., Lindsey, G., Marshall, J.D., 2017. Population-level exposure to particulate air pollution during active travel: planning for low-exposure, health-promoting cities. *Environ. Health Perspect.* 125, 527–534.
- Harkey, D.L., Reinfort, D.W., Knuiman, M., Stewart, J.R., Sorton, A., 1998. Development of the Bicycle Compatibility Index: A Level of Service Concept, Final Report, United States. Federal Highway Administration.
- Hatzopoulou, M., Weichenthal, S., Dugum, H., Pickett, G., Miranda-Moreno, L., Kulka, R., Andersen, R., Goldberg, M., 2013. The impact of traffic volume, composition, and road geometry on personal air pollution exposures among cyclists in Montreal, Canada. *J. Exposure Sci. Environ. Epidemiol.* 23, 46–51.
- Jacobs, A., Appleby, D., 1987. Toward an urban design manifesto. *J. Am. Plan. Assoc.* 53, 112–120.
- Kang, H., Kim, D.H., Yoo, S., 2019. Attributes of perceived bikeability in a compact urban neighborhood based on qualitative multi-methods. *Int. J. Environ. Res. Public Health* 16, 3738.
- Kaur, S., Nieuwenhuijsen, M.J., Colvile, R.N., 2007. Fine particulate matter and carbon monoxide exposure concentrations in urban street transport microenvironments. *Atmos. Environ.* 41, 4781–4810.
- Keall, M.D., Shaw, C., Chapman, R., Howden-Chapman, P., 2018. Reductions in carbon dioxide emissions from an intervention to promote cycling and walking: a case study from New Zealand. *Transp. Res. Part D: Transp. Environ.* 65, 687–696.
- Koh, P., Wong, Y., 2013. Influence of infrastructural compatibility factors on walking and cycling route choices. *J. Environ. Psychol.* 36, 202–213.
- Koh, P., Wong, Y.D., 2015. Proceedings of the Institution of Civil Engineers-Municipal Engineer, Thomas Telford Ltd, pp. 106–114.
- Krabbenborg, L., 2015. *Cycling to a Railway Station: Exploring the Influence of the Urban Environment on Travel Resistance*. Master's Thesis. University of Technology Delft.

- Krenn, P.J., Oja, P., Titze, S., 2015. Development of a bikeability index to assess the bicycle-friendliness of urban environments. *Open J. Civil Eng.* 5, 451.
- Krzyżanowski, M., Kuna-Dibbert, B., Schneider, J., 2005. Health Effects of Transport-Related Air Pollution. WHO Regional Office Europe.
- Lin, J.-J., Wei, Y.-H., 2018. Assessing area-wide bikeability: a grey analytic network process. *Transp. Res. Part A: Policy Pract.* 113 (C), 381–396.
- Lin, J.-J., Zhao, P., Takada, K., Li, S., Yai, T., Chen, C.-H., 2018. Built environment and public bike usage for metro access: a comparison of neighborhoods in Beijing, Taipei, and Tokyo. *Transp. Res. Part D: Transp. Environ.* 63, 209–221.
- Liu, P., Zhao, C., Göbel, T., Hallbauer, E., Nowak, A., Ran, L., Xu, W., Deng, Z., Ma, N., Mildnerger, K., 2011. Hygroscopic properties of aerosol particles at high relative humidity and their diurnal variations in the North China plain. *Atmos. Chem. Phys.* 11, 3479–3494.
- Lovelace, R., Goodman, A., Aldred, R., Berkoff, N., Abbas, A., Woodcock, J., 2017. The propensity to cycle tool: an open source online system for sustainable transport planning. *J. Transp. Land Use* 10, 505–528.
- LTA, 2017. Road Network. Land Transport Authority.
- LTA, 2018. Land Transport Master Plan 2040, Land Transport Authority.
- LTA, 2019a. Bus Stop Location. Land Transport Authority., LTA Data Mall.
- LTA, 2019b. Cycling Routes. Land Transport Authority.
- Marquart, H., Schlink, U., Ueberham, M., 2020. The planned and the perceived city: a comparison of cyclists' and decision-makers' views on cycling quality. *J. Transp. Geogr.* 82, 102602.
- Marshall, J.D., Nethery, E., Brauer, M., 2008. Within-urban variability in ambient air pollution: comparison of estimation methods. *Atmos. Environ.* 42, 1359–1369.
- Meng, M., Koh, P., Wong, Y., Zhong, Y., 2014. Influences of urban characteristics on cycling: experiences of four cities. *Sustainable Cities Soc.* 13, 78–88.
- Meng, M., Zhang, J., Wong, Y., Au, P., 2016. Effect of weather conditions and weather forecast on cycling travel behavior in Singapore. *Int. J. Sustainable Transp.* 10, 773–780.
- Menon, S., Hansen, J., Nazarenko, L., Luo, Y., 2002. Climate effects of black carbon aerosols in China and India. *Science* 297, 2250–2253.
- Minet, L., Gehr, R., Hatzopoulou, M., 2017. Capturing the sensitivity of land-use regression models to short-term mobile monitoring campaigns using air pollution micro-sensors. *Environ. Pollut.* 230, 280–290.
- Minet, L., Liu, R., Valois, M.-F., Xu, J., Weichenthal, S., Hatzopoulou, M., 2018a. Development and comparison of air pollution exposure surfaces derived from on-road mobile monitoring and short-term stationary sidewalk measurements. *Environ. Sci. Technol.* 52, 3512–3519.
- Minet, L., Stokes, J., Scott, J., Xu, J., Weichenthal, S., Hatzopoulou, M., 2018b. Should traffic-related air pollution and noise be considered when designing urban bicycle networks? *Transp. Res. Part D: Transp. Environ.* 65, 736–749.
- Moran, P.A., 1950. Notes on continuous stochastic phenomena. *Biometrika* 37, 17–23.
- MOT, 2020. Achieving Cleaner Transport, <https://www.mot.gov.sg/About-MOT/Land-Transport/Sustainable-Transport/Achieving-Cleaner-Transport/>, Last Access: 5 July 2020.
- MTI, 2016. Singapore Residents by Subzone and Type of Dwelling, June 2016, Ministry of Trade and Industry - Department of Statistics (Ed.), Data.gov.sg.
- Muhs, C.D., Clifton, K.J., 2016. Do characteristics of walkable environments support bicycling? Toward a definition of bicycle-supported development. *J. Transp. Land Use* 9, 147–188.
- Mulley, C., Tyson, R., McCue, P., Rissel, C., Munro, C., 2013. Valuing active travel: including the health benefits of sustainable transport in transportation appraisal frameworks. *Res. Transp. Bus. Manage.* 7, 27–34.
- Nguyen, T., Lechner, B., Wong, Y.D., Tan, J.Y., 2019a. Bus ride index—a refined approach to evaluating road surface irregularities. *Road Mater. Pavement Des.* 1–21.
- Nguyen, T., NguyenDinh, N., Lechner, B., Wong, Y.D., 2019b. Insight into the lateral ride discomfort thresholds of young-adult bus passengers at multiple postures: case of Singapore. *Case Stud. Transp. Policy* 7, 617–627.
- Nielsen, T.A.S., Skov-Petersen, H., 2018. Bikeability-urban structures supporting cycling. Effects of local, urban and regional scale urban form factors on cycling from home and workplace locations in Denmark. *J. Transp. Geogr.* 69, 36–44.
- Porter, A.K., Kohl III, H.W., Pérez, A., Reininger, B., Pettee Gabriel, K., Salvo, D., 2019. Bikeability: assessing the objectively measured environment in relation to recreation and transportation bicycling. *Environ. Behav.* 0013916518825289.
- Pritchard, R., Frøyen, Y., Snizek, B., 2019. Bicycle level of service for route choice—a gis evaluation of four existing indicators with empirical data. *ISPRS Int. J. Geo-Inf.* 8, 214.
- Qiu, Z., Wang, W., Zheng, J., Lv, H., 2019. Exposure assessment of cyclists to ufp and pm on urban routes in Xi'an, China. *Environ. Pollut.* 250, 241–250.
- Raza, W., Forsberg, B., Johansson, C., Sommar, J.N., 2018. Air pollution as a risk factor in health impact assessments of a travel mode shift towards cycling. *Global Health Action* 11, 1429081.
- Rizzo, L.V., Artaxo, P., Mueller, T., Wiedensohler, A., Paixao, M., Cirino, G.G., Arana, A., Swietlicki, E., Roldin, P., Fors, E.O., 2013. Long term measurements of aerosol optical properties at a primary forest site in amazonia. *Atmos. Chem. Phys.* 13, 2391–2413.
- Ryu, J., Jung, J.H., Kim, J., Kim, C.-H., Lee, H.-B., Kim, D.-H., Lee, S.-K., Shin, J.-H., Roh, D., 2020. Outdoor cycling improves clinical symptoms, cognition and objectively measured physical activity in patients with schizophrenia: a randomized controlled trial. *J. Psychiatr. Res.* 120, 144–153.
- Saghapour, T., Moridpour, S., Thompson, R.G., 2017. Measuring cycling accessibility in metropolitan areas. *Int. J. Sustainable Transp.* 11, 381–394.
- Sharma, A.R., Kharol, S.K., Badarinath, K., 2010. Influence of vehicular traffic on urban air quality—a case study of Hyderabad, India. *Transp. Res. Part D: Transp. Environ.* 15, 154–159.
- Smith, M., Hosking, J., Woodward, A., Witten, K., MacMillan, A., Field, A., Baas, P., Mackie, H., 2017. Systematic literature review of built environment effects on physical activity and active transport—an update and new findings on health equity. *Int. J. Behav. Nutrit. Phys. Activity* 14, 158.
- Su, S., Zhou, H., Xu, M., Ru, H., Wang, W., Weng, M., 2019. Auditing street walkability and associated social inequalities for planning implications. *J. Transp. Geogr.* 74, 62–76.
- Sun, G., Zhao, J., Webster, C., Lin, H., 2020. New metro system and active travel: a natural experiment. *Environ. Int.* 138, 105605.
- Tan, S.H., Roth, M., Velasco, E., 2017. Particle exposure and inhaled dose during commuting in Singapore. *Atmos. Environ.* 170, 245–258.
- Terh, S.H., Cao, K., 2018. Gis-Mcda based cycling paths planning: a case study in Singapore. *Appl. Geogr.* 94, 107–118.
- Tran, P.T., Ngoh, J.R., Balasubramanian, R., 2020a. Assessment of the integrated personal exposure to particulate emissions in urban micro-environments: a pilot study. *Aerosol Air Qual. Res.* 20, 341–357.
- Tran, P.T., Nguyen, T., Balasubramanian, R., 2020b. Personal exposure to airborne particles in transport micro-environments, potential health impacts: a tale of two cities. *Sustainable Cities Soc.*, 102470.
- Ueberham, M., Schlink, U., Dijst, M., Weiland, U., 2019. Cyclists' multiple environmental urban exposures—comparing subjective and objective measurements. *Sustainability* 11, 1412.
- URA, 2014. Master Plan 2014 Land Use. Urban Redevelopment Authority, Data.gov.sg.
- USGS, 2020. Digital Elevation Model Dataset.
- Van den Bossche, J., De Baets, B., Verwaeren, J., Botteldooren, D., Theunis, J., 2018. Development and evaluation of land use regression models for black carbon based on bicycle and pedestrian measurements in the urban environment. *Environ. Modell. Software* 99, 58–69.
- Van den Hove, A., Verwaeren, J., Van den Bossche, J., Theunis, J., De Baets, B., 2019. Development of a land use regression model for black carbon using mobile monitoring data and its application to pollution-avoiding routing. *Environ. Res.*, 108619.
- Van Dyck, D., Cerin, E., Conway, T.L., De Bourdeaudhuij, I., Owen, N., Kerr, J., Cardon, G., Frank, L.D., Saelens, B.E., Sallis, J.F., 2012. Perceived neighborhood environmental attributes associated with adults' transport-related walking and cycling: findings from the USA, Australia and Belgium. *Int. J. Behav. Nutrit. Phys. Activity* 9, 70.
- Vedel, S.E., Jacobsen, J.B., Skov-Petersen, H., 2017. Bicyclists' preferences for route characteristics and crowding in Copenhagen—a choice experiment study of commuters. *Transp. Res. Part A: Policy Pract.* 100, 53–64.
- Wahlgren, L., Schantz, P., 2012. Exploring Bikeability in a metropolitan setting: stimulating and hindering factors in commuting route environments. *BMC Public Health* 12, 168.

- WHO, 2020. Ambient (Outdoor) Air Pollution, [https://www.who.int/news-room/fact-sheets/detail/ambient-\(outdoor\)-air-quality-and-health](https://www.who.int/news-room/fact-sheets/detail/ambient-(outdoor)-air-quality-and-health), Last Access: 6 July 2020.
- Winters, M., Brauer, M., Setton, E.M., Teschke, K., 2013. Mapping bikeability: a spatial tool to support sustainable travel. *Environ. Plan. B: Plan. Des.* 40, 865–883.
- Winters, M., Teschke, K., Brauer, M., Fuller, D., 2016. Bike Score®: associations between urban bikeability and cycling behavior in 24 cities. *Int. J. Behav. Nutrit. Phys. Activity* 13, 18.
- Woodcock, J., Edwards, P., Tonne, C., Armstrong, B.G., Ashiru, O., Banister, D., Beevers, S., Chalabi, Z., Chowdhury, Z., Cohen, A., 2009. Public health benefits of strategies to reduce greenhouse-gas emissions: urban land transport. *The Lancet* 374, 1930–1943.
- Wu, X., Lu, Y., Lin, Y., Yang, Y., 2019. Measuring the destination accessibility of cycling transfer trips in metro station areas: a big data approach. *Int. J. Environ. Res. Public Health* 16, 2641.
- Yang, S., Wu, H., Chen, J., Lin, X., Lu, T., 2018. Optimization of Pm2. 5 estimation using landscape pattern information and land use regression model in Zhejiang, China. *Atmosphere* 9, 47.
- Zahabi, S.A.H., Chang, A., Miranda-Moreno, L.F., Patterson, Z., 2016. Exploring the link between the neighborhood typologies, bicycle infrastructure and commuting cycling over time and the potential impact on commuter ghg emissions. *Transp. Res. Part D: Transp. Environ.* 47, 89–103.
- Zhang, Y., Thomas, T., Brussel, M., Van Maarseveen, M., 2017. Exploring the impact of built environment factors on the use of public bikes at bike stations: case study in Zhongshan, China. *J. Transp. Geogr.* 58, 59–70.
- Zhang, Z., Ming, Y., Song, G., 2019. Identify road clusters with high-frequency crashes using spatial data mining approach. *Appl. Sci.* 9, 5282.
- Zhao, J., Wang, J., Deng, W., 2015. Exploring bikesharing travel time and trip chain by gender and day of the week. *Transp. Res. Part C: Emerg. Technol.* 58, 251–264.
- Zhao, P., 2014. The impact of the built environment on bicycle commuting: evidence from Beijing. *Urban Stud.* 51, 1019–1037.
- Zhao, P., Li, S., Li, P., Liu, J., Long, K., 2018. How does air pollution influence cycling behaviour? Evidence from Beijing. *Transp. Res. Part D: Transp. Environ.* 63, 826–838.
- Zhou, H., He, S., Cai, Y., Wang, M., Su, S., 2019. Social inequalities in neighborhood visual walkability: using street view imagery and deep learning technologies to facilitate healthy city planning. *Sustainable Cities Soc.* 50, 101605.
- Zhu, S., Zhu, F., 2019. Cycling comfort evaluation with instrumented probe bicycle. *Transp. Res. Part A: Policy Pract.* 129, 217–231.